FAIRSEA (ID 10046951)

"Fisheries in the AdriatIc Region - a Shared Ecosystem Approach"

D 4.2.2 – Future scenarios of production patterns

Work Package:	WP4 **Implementation of a shared and integrated platform** Activity: 4.2 - **BGC – Biogeochemical processes and dynamics**
Type of Document	A report and a database on the space-time distribution of nitrogen, chlorophyll, primary production, plankton biomass and oxygen indicators in the 21st century under emission scenarios RCP4.5 and RCP8.5
Use	Public
Responsible PP	OGS
Authors	Gianpiero Cossarini (GC), Marco Reale (MR)
Version and date	Version 1, 08/01/2021

Deliverable 4.2.2

Future scenarios of production patterns

FAIRSEA – Fisheries in the Adriatic Region – a shared Ecosystem Approach

FAIRSEA is financed by Interreg V-A IT-HR CBC Programme (Priority Axis 1 – Blue innovation)

Start date: 01 January 2019
End date: 28 February 2021

Contents

Acronyms used

BFM	Biogeochemical Flux Model
CMCC	Centro Euro-Mediterraneo per i Cambiamenti Climatici
DIC	Dissolved Inorganic Carbon
DIN	Dissolved Nitrogen
EAF	Ecosystem Approach to Fisheries
EAFM	Ecosystem Approach to Fisheries Management
FAIRSEA	Fisheries in the Adrlatic Region – a Shared Ecosystem Approach
GSA	FAO Geographical Sub Areas
KoM	Kick-off Meeting
MFS	Mediterranean Forecasting System
NEMO	Nucleous for European Modelling of the Ocean
NetCDF	Network Common Data Form
OGS	Istituto Nazionale di Oceanografia e di Geofisica Sperimentale
OGSTM	OGS - Transport Model
PFT	Plankton Functional Types
WP	Work packages

Introduction

This report presents a description of the biogeochemical properties of the Adriatic and Ionian basins in the 21st century (the physical properties are described in D 4.1.2) under emission scenarios RCP4.5 and RCP8.5 (IPCC, 2014: AR5). The analysis is based on two datasets, spanning the 2005-2100 time period, provided by the offline coupling between the physical MFS16 (Oddo et al., 2009; Cavicchia et al., 2011) and the transport-biogeochemical OGSTM-BFM (Lazzari et al., 2012; 2016; Cossarini et al., 2015) models. Results of the scenario simulations cover the entire Mediterranean Sea and have a spatial resolution of 1/16° in the horizontal direction, while the vertical discretization considers 70 unevenly-spaced levels. The datasets have been produced by OGS (www.inogs.it) using the computational resources available at the CINECA supercomputing center (www.cineca.it). Data and figures of the present deliverable have been, respectively, reprocessed and generated specifically for the Adriatic and Ionian basins.

The evolution of the biogeochemical conditions in the 21st century under the proposed scenarios integrates analysis of the present-day conditions provided in deliverable 4.2.1. Given the consistency of the models and the domain of both the reanalysis and scenario simulations, the anomalies provided in the present report can be combined (summed) to the mean concentration values of the present-day condition (provided in D 4.2.1) to obtain the projected concentration values of the biogeochemical variables in the 21st century.

The MFS16/OGSTM-BFM modelling system: the biogeochemical component

The present deliverable is the companion of deliverable D 4.1.2, describing the MFS16/OGSTM-BFM physical-biogeochemical modelling system. Only a brief summary of the MFS16/OGSTM-BFM is depicted hereafter, focusing on its biogeochemical component.

The integrated physical-biogeochemical dataset covers the period 2005-2100. Data have a spatial resolution of 1/16°, which satisfies the requirements of the other WPs relying on hydrodynamic/biogeochemical output fields. Model domain is composed of 70 unevenly-spaced vertical levels at the depth of (from surface to bottom, in meters): 1.5, 4.6, 8.0, 11.6, 15.5, 19.6, 24.1, 29.0, 34.2, 39.7, 45.7, 52.2, 59.1, 66.4, 74.4, 82.9, 92.0, 102, 112, 124, 136, 148, 162, 177, 193, 210, 228, 247, 268, 290, 313, 339, 366, 395, 426, 458, 494, 532, 572, 615, 661, 710, 763, 819, 878, 943, 1011, 1084, 1162, 1245, 1334, 1428, 1529, 1637, 1751, 1874, 2004, 2143, 2291, 2448, 2616, 2795, 2985, 3187, 3402, 3631, 3874, 4132, 4406, 4698.

The integrated dataset includes monthly fields of fourteen 3D variables and three 2D variables. Three dimensional variables are temperature, salinity, meridional and zonal currents, chlorophyll-a, nitrate, phosphate, dissolved oxygen, phytoplankton carbon biomass, pCO_2, alkalinity, pH and net primary production. The two dimensional variables are sea surface height, bottom values of temperature and bottom values of oxygen. The model domain encompasses the Mediterranean Basin (8.81°W-36.25°E and 30.1875°N-45.9375°N) and part of the Atlantic Ocean, in order to better resolve the exchanges at the Strait of Gibraltar. The MFS16 model computes the air-sea fluxes of water, momentum and heat using specific bulk formulae tuned for the Mediterranean Sea (see details in Oddo et al., 2009) applied to the results of the atmospheric model CMCC-CM (extensively

described in Scoccimarro et al., 2011). Moreover, a bias correction is applied to the atmospheric fields based on a 3-step stepwise procedure that uses the ERA-Interim dataset (Dee et al., 2011). The three steps are: re-gridding of ERA-interim fields on the CMCC-CM grid, computation of monthly biases between CMCC-CC model and ERA-Interim reanalysis for the present condition and, finally, addition of the biases to the original fields produced by the climate model. The biogeochemical data are produced using the OGSTM-BFM modeling system which is based on the transport model OGSTMv2.0 and the biogeochemical reactor Biogeochemical Flux Model BFMv5 (Lazzari et al., 2012, 2016; Cossarini et al., 2015, and references therein).

The physical model (described in D 4.1.2) provides the transport-biogeochemical OGSTM-BFM model with the temporal evolution of daily 3D fields of horizontal and vertical current velocities, vertical eddy diffusivity, potential temperature, salinity, in addition to surface data for solar shortwave irradiance and wind stress. The transport-biogeochemical reactor simulates the dynamics of nine plankton functional types (4 phytoplankton functional groups: diatoms, flagellates, picophytoplankton and dinoflagellates; four zooplankton groups; one bacteria), the biogeochemical cycles of 5 chemical compounds (carbon, nitrogen, phosphorus, silica, and oxygen) through the dissolved inorganic, living organic and non-living organic compartments, and the carbonate system resolving the dynamics of pCO_2, acidity and carbon pump.

Two future emission scenarios, RCP4.5 and RCP8.5 (Moss et al., 2010), are used to force the atmospheric module of the CMCC-CM model and subsequently the coupled physical-biogeochemical MFS16-OGSTM-BFM model of the Mediterranean Sea. In particular, the RCP4.5 represents an intermediate scenario where CO2 emissions peak around 2040 (causing the maximum increase in CO2 concentration, Fig. 1), then decline (with a resulting plateau in the CO2 concentration). As a consequence, at the end of the 21st century, the atmospheric pCO_2 will be around 560-580 ppm (Fig.1) and atmospheric

temperature will increase of 1.8 (1.1 to 2.6)°C with respect the present-day condition. In the worst-case scenario RCP8.5, the CO_2 emissions will continue to rise throughout the 21st century, the pCO_2 concentration will rise to 1200 ppm (Fig. 1) at the end of the 21st century, and the temperature increase will be of 3.7 (2.6 to 4.8)°C (IPCC, 2014: AR5).

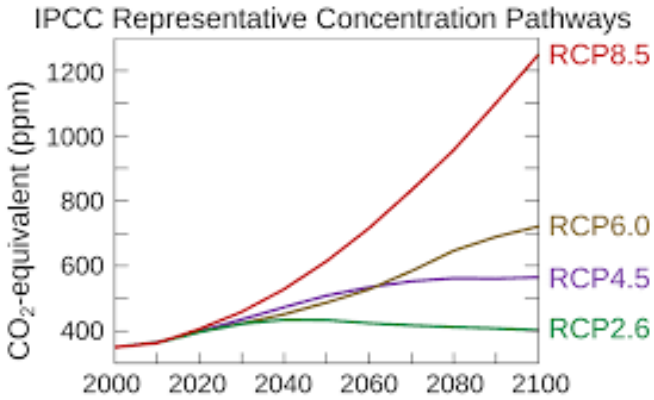

Figure 1 - Atmospheric pCO_2 concentration under different future scenarios used for the climate modeling of the IPCC fifth Assessment Report
(From: https://en.wikipedia.org/wiki/Representative_Concentration_Pathway; data: IPCC, 2014 - AR5)

Methodology for the future scenario analysis

A specific simulation and analysis protocol has been implemented in order to disentangle the climate change signal from the spurious signal due to the inaccuracies of the numerical model. In fact, long term biogeochemical simulations can be affected by errors related to the numerical accuracy and the not perfectly balanced set up of boundary conditions, transport process and internal element cycle formulations of the biogeochemical model. Errors can accumulate during the simulation, generating drifts in the evolution of the variables that can overlap and partially hide the climate signals. Thus, the protocol consists of two 100-years simulations: one reproducing repeatedly an average condition (i.e., control simulation, hereafter CTRL) and a second one reproducing the climate scenario. In particular, the control run consists of a simulation performed by using the forcing of the period 2005-2014 looped over the entire time period of the simulation (2005-2100). The difference between the two simulations provides the evolution of the variable due to the future climate forcing (Fig. 2).

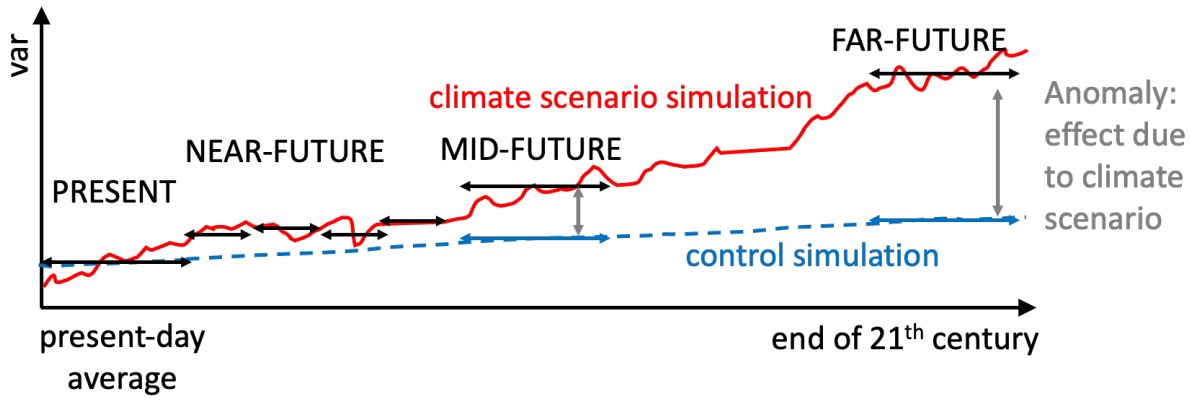

Figure 2 - Scheme of the simulation and analysis protocol.

In the analysis phase, being X a 3D monthly variable, we computed its annual timeseries X_k with k=2005, ..., 2099 considering the following vertical averaged layers: 0-50 m, 50-100 m, 100-200 m, 200-500 m and 500-800 m. Then we defined for each X_k the following variable $X\_Evo_{SCEN,k}$ (with k=2005, ..., 2099) as:

$$X\_Evo_{SCEN,k} = [X_{SCEN,k} - X_{CTRL,k}] \quad (1)$$

where $X_{SCEN,k}$ and $X_{CTRL,k}$ are the annual timeseries of X_k for the climate scenario (i.e., RCP4.5 or RCP8.5) and the control simulation (CTRL), respectively. Hereafter, if not differently reported, all the mean annual concentration timeseries presented refer to $X\_Evo_{SCEN,k}$. In the order to point out the variation of each variable X with respect to the present climate state period (2005-2020, hereafter PRESENT) the following periods have been selected: four 5-year periods 2021-2025, 2026-2030, 2031-2035, 2036-2040 (hereafter NEAR-FUTURE), and two 20-year periods 2040-2059 (hereafter MID-FUTURE) and 2080-2099 (hereafter FAR-FUTURE). Moreover we introduced the quantity X_ANOM_{period}. More specifically being the period chosen for example MID-FUTURE or FAR-FUTURE (both will be discussed in this deliverable as they are 20-years-long periods which allow for a robust average computation removing the effects of the interannual variability) the anomaly of the two periods with respect to the PRESENT are named as $X\_ANOM_{MID\text{-}FUTURE}$ and $X\_ANOM_{FAR\text{-}FUTURE}$, respectively, and computed as:

$$X\_ANOM_{MID\text{-}FUTURE} = Evo_{X\_SCEN\text{-}MID\text{-}FUTURE} - Evo_{X\_SCEN\text{-}PRESENT} \quad (2)$$

$$X\_ANOM_{FAR\text{-}FUTURE} = Evo_{X\_SCEN\text{-}FAR\text{-}FUTURE} - Evo_{X\_SCEN\text{-}PRESENT} \quad (3)$$

where $Evo_{X\_SCEN\text{-}MID\text{-}FUTURE}$, $Evo_{X\_SCEN\text{-}FAR\text{-}FUTURE}$ and $Evo_{X\_SCEN\text{-}PRESENT}$ are the averages of the annual means of the scenario ($Evo_{X\_SCEN,k}$) for the MID-FUTURE, FAR-FUTURE and PRESENT periods, respectively. Hereafter, if not differently specified, all the mean concentrations shown later in the maps will be represented by X_ANOM.

The analysis of the future scenario is integrated by the time series of the annual anomalies computed as:

$$<X\_ANOM_k> = <Evo_{x\_SCEN,k}> - < Evo_{X\_SCEN-PRESENT} > \quad (4)$$

where < > represents the spatial average calculated over the three GSA areas and the inshore (area shallower than 200 m) and off-shore (area deeper than 200m) zones.

It is worth to note that the climate scenario anomalies (timeseries and reference period maps presented in the next sections) can be used conjunctly with the assessment of the present-day condition (deliverable D 4.2.1) to eventually reconstruct the future actual values of the biogeochemical variables. Indeed, given the consistency of the models domain configuration between reanalysis (deliverable D 4.2.1) and climate simulations (present deliverable), the layers of the future scenario anomalies can be directly combined with the layers of the present-day average conditions in the FAIRSEA web portal.

Biogeochemical characteristics of the Adriatic Sea and Northern Ionian Sea in the future climate scenarios (GSA 17-18-19)

In this section we analyze the spatial patterns and temporal behavior of the biogeochemical properties in the Adriatic and Ionian systems in future climate under emission scenarios RCP4.5 and RCP8.5, with a specific focus on the period 2040-2059 (hereafter MID-FUTURE) and 2080-2099 (hereafter FAR-FUTURE).

Dissolved Nitrogen

Figures 3 and 4 shows the mean annual anomalies of dissolved inorganic nitrogen (DIN) for the MID-FUTURE period with respect the PRESENT under the emission scenarios RCP4.5 and RCP8.5, respectively. The FAR-FUTURE anomalies for the two scenarios are shown in the Figures 5 and 6. The distribution of DIN anomalies shows a substantial increase in the concentration in the relatively shallow northern Adriatic and along the Italian coast and a general decrease in all off-shore areas of the Adriatic and Ionian Sea in MID-FUTURE of both scenarios. Coastal increases are mainly due to changes in basin circulation. It is worth to remind that nutrient loads from rivers of the future scenario are set constant and equal to the present-day condition. At the present stage, no information on the evolution of the nutrient loads in the Mediterranean region for the 21st century are available.

An increase in the vertical stratification of the water column is responsible for the negative anomaly observed in the Southern Adriatic Sea and only partially in the Ionian Sea, where in turn, we observed a slight increase in the concentration of nutrient in the southern part mostly influenced with the inflow of Atlantic water.

At the end of the 21st century, an increase of nitrogen concentration is simulated in both scenarios (stronger in RCP8.5) below 500 m due to the accumulation of the nutrient which is less efficiently transported upwards by the vertical winter mixing processes.

The time-series of the mean spatial DIN anomalies for inshore (Fig. 7) and offshore (Fig. 8) areas in RCP4.5 (left panel) and RCP8.5 (right panel) scenarios are shown for the three GSA areas: Northern Adriatic (SGA17), Southern Adriatic (GSA18) and Ionian (GSA19). Surface concentration of DIN does not present any significant long term changes in both inshore and offshore areas for the three GSA areas. Below the surface,

all three areas show a decline after 2030, which is more remarkable in the Adriatic Sea and, in particular, in the offshore areas.

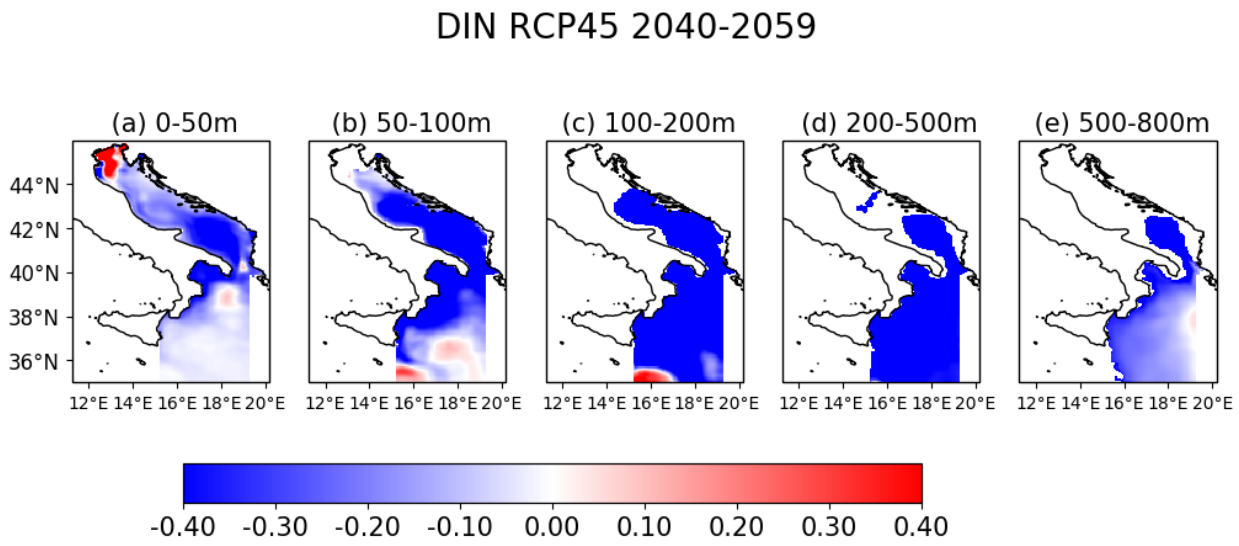

Figure 3 - Mean dissolved inorganic nitrogen (DIN) anomaly (mmol/m^3) in the MID-FUTURE of the RCP4.5 scenario in the five layers: 0-50 m, 50-100 m, 100-200 m, 200-500 m and 500-800 m

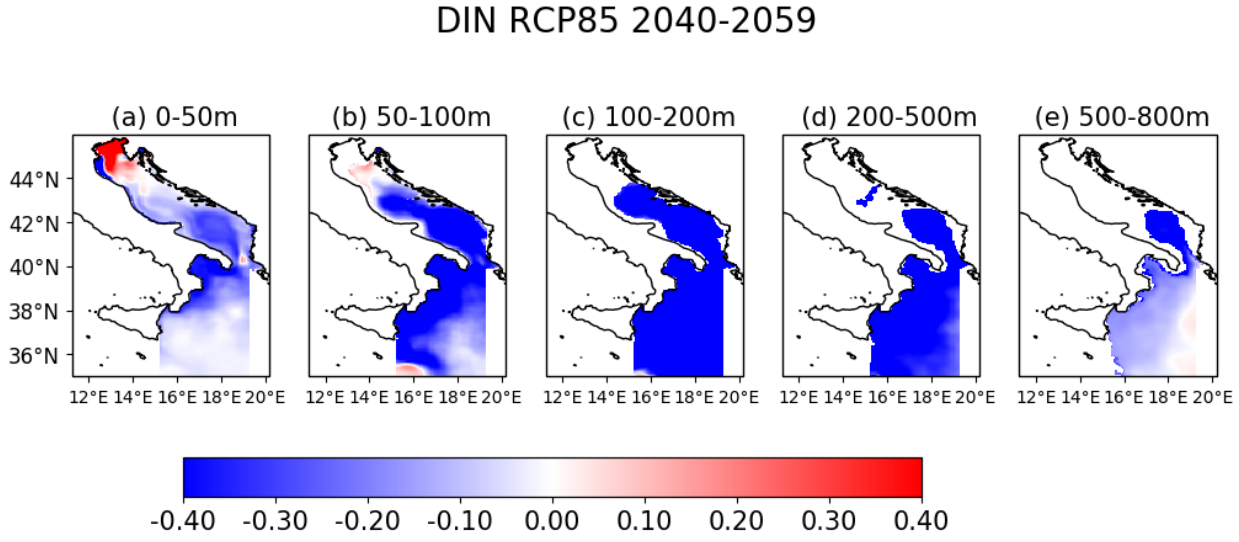

Figure 4 - Mean dissolved inorganic nitrogen (DIN) anomaly (mmol/m^3) in the MID-FUTURE of the RCP8.5 scenario in the five layers: 0-50 m, 50-100 m, 100-200 m, 200-500 m and 500-800 m

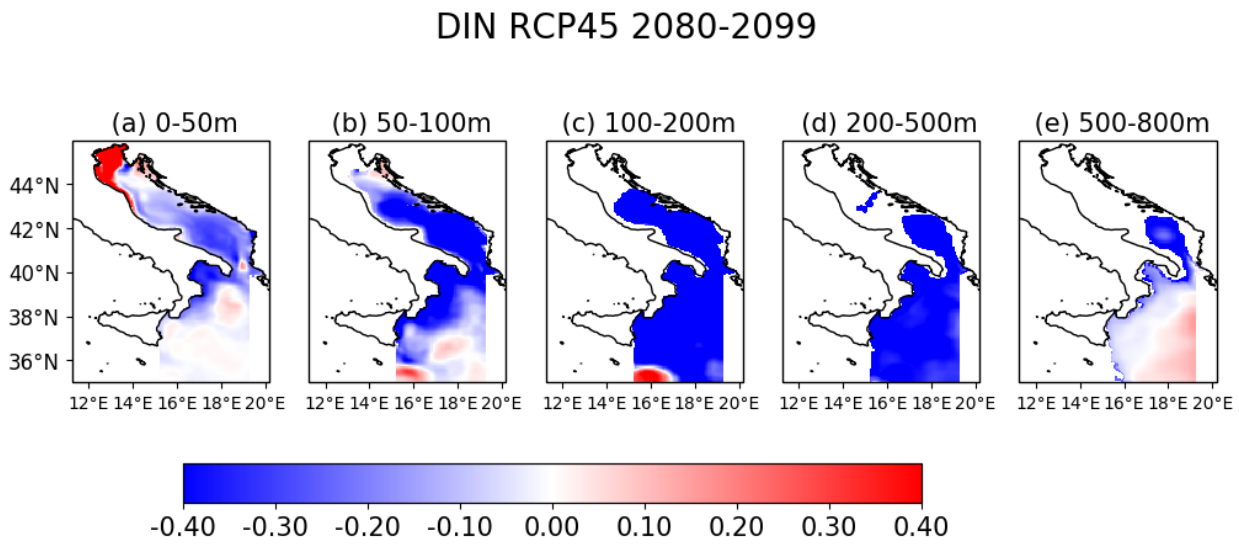

Figure 5 - Mean dissolved inorganic nitrogen (DIN) anomaly (mmol/m^3) in the FAR-FUTURE of the RCP4.5 scenario in the five layers: 0-50 m, 50-100 m, 100-200 m, 200-500 m and 500-800 m

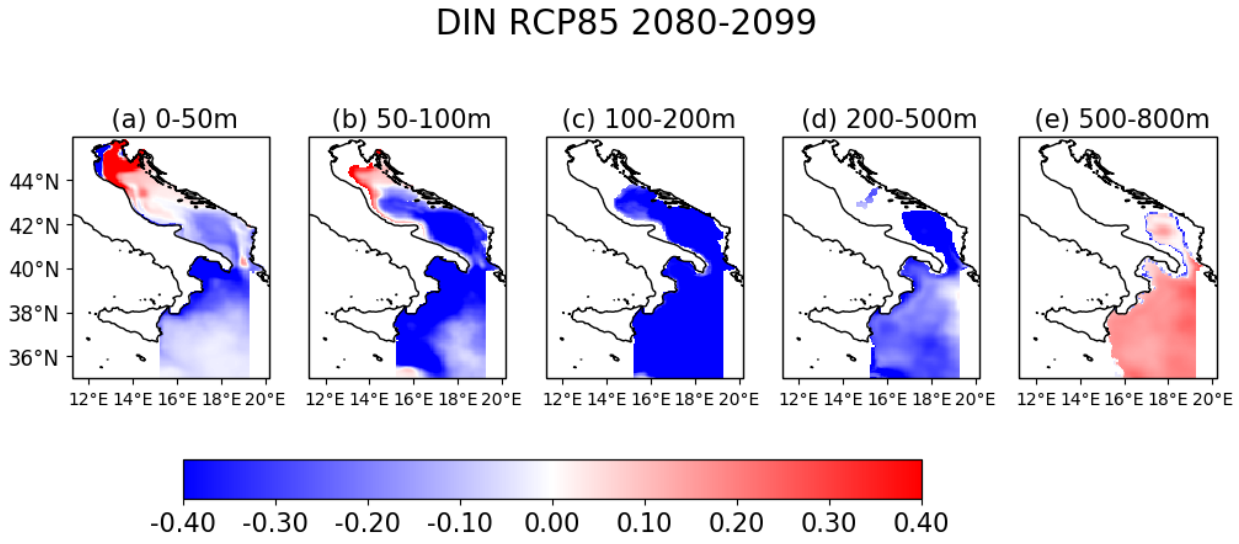

Figure 6 - Mean dissolved inorganic nitrogen (DIN) anomaly (mmol/m^3) in the FAR-FUTURE of the RCP8.5 scenario in the five layers: 0-50 m, 50-100 m, 100-200 m, 200-500 m and 500-800 m

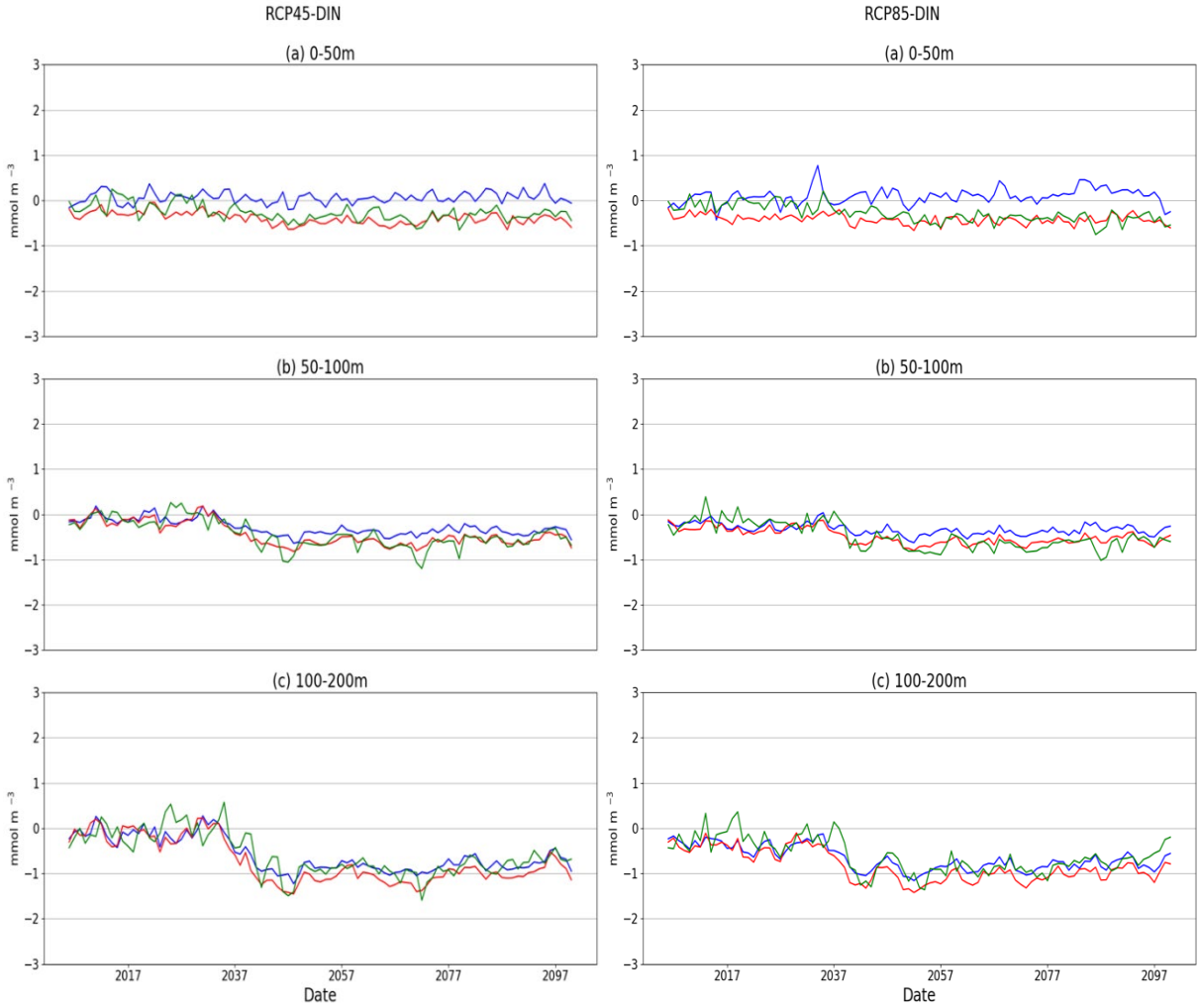

Figure 7 - Annual timeseries of dissolved inorganic nitrogen anomalies (mmol/m^3) in the three inshore (depth less than 200 m) areas of the Adriatic-Ionian Sea: GSA17 - northern Adriatic (blue), GSA18 - southern Adriatic (red) and GSA19 - Ionian (green). Timeseries cover the 2005-2099 period for the two emission RCP4.5 (left) and RCP8.5 (right) scenarios.

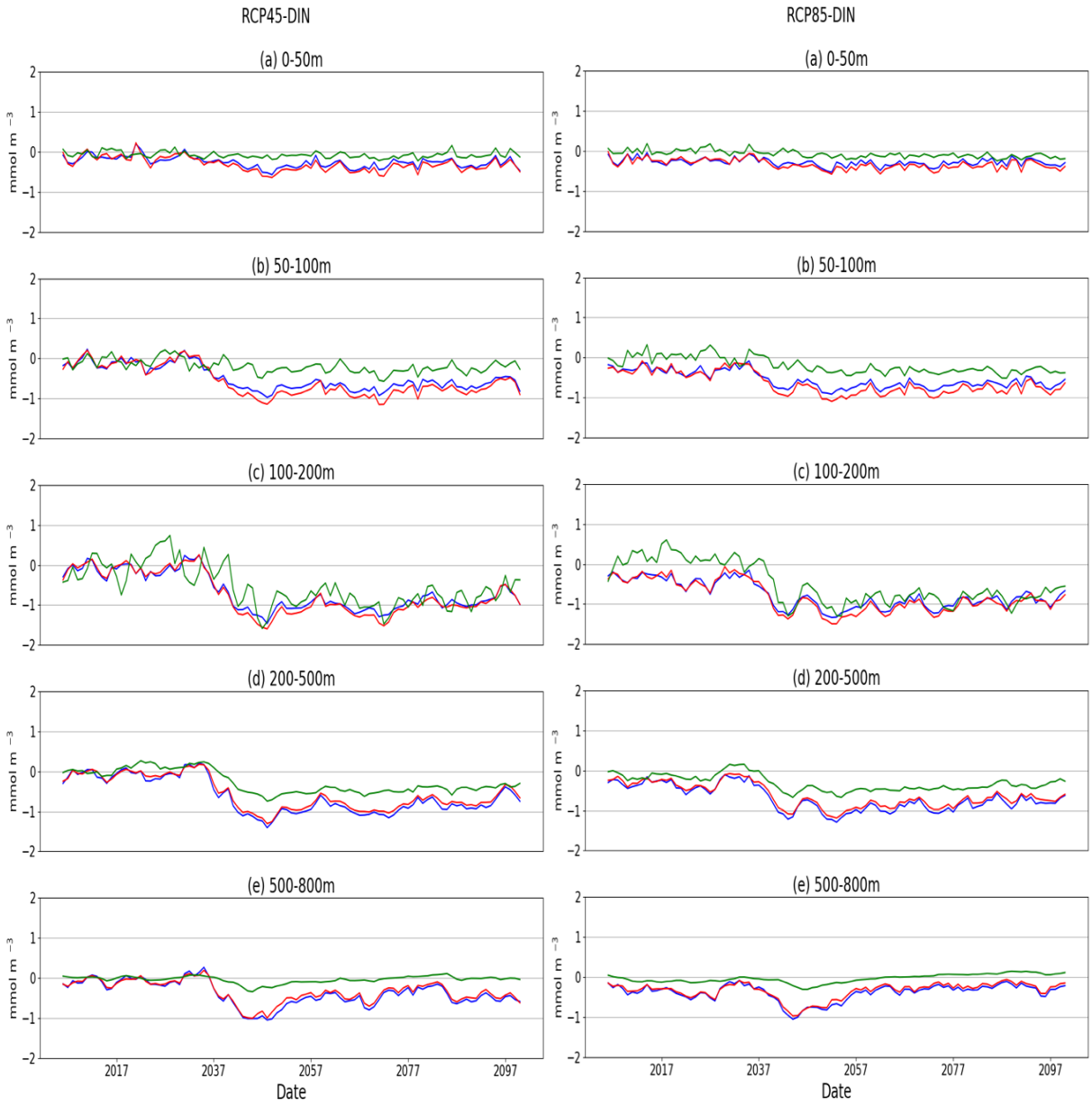

Figure 8 - Annual timeseries of dissolved inorganic nitrogen anomalies (mmol/m^3) in the three offshore (deeper than 200 m) areas of the Adriatic-Ionian Sea: GSA17 - northern Adriatic (blue), GSA18 - southern Adriatic (red) and GSA19 - Ionian (green). Timeseries cover the 2005-2099 period for the two emission RCP4.5 (left) and RCP8.5 (right) scenarios.

Phosphate

Phosphate (PO_4) anomalies computed for the MID-FUTURE and FAR-FUTURE under the two emission scenarios are shown in the maps of Figs. 9-12. Phosphorus is considered the limiting nutrient for phytoplankton growth in the Mediterranean Sea (Lazzari et al., 2016). The distribution of surface phosphate anomalies (0-50 m) shows some similarities with that observed for the DIN: a slight increase of concentration in the northernmost part of the Adriatic sea and a widespread decrease in the offshore Adriatic Sea and Ionian Seas in the MID-FUTURE. A decrease of concentration of phosphate below the surface in both scenarios is shown for the MID-FUTURE (Fig. 9 and 10) while an accumulation of phosphate in the 500-800 m layer of the Ionian is foreseen at the end of the century of the RCP8.5 scenario. As already observed for DIN, the decrease of phosphate in the intermediate layers of the Adriatic-Ionian basin takes place mainly after 2030 (Figs.13-14) in both inshore and offshore areas.

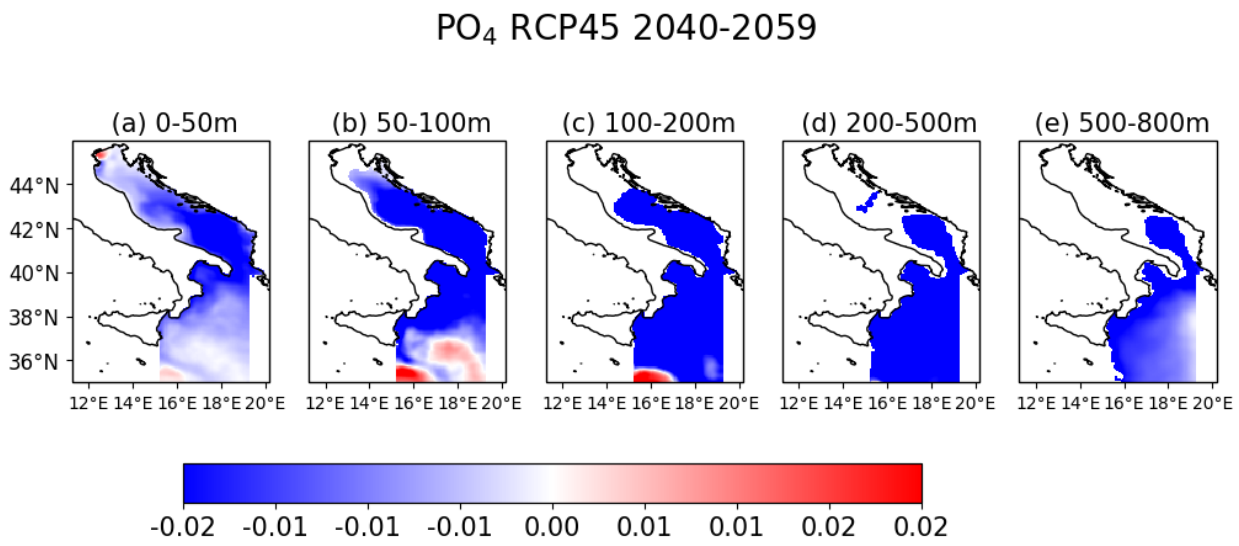

Figure 9 - Mean phosphate (PO_4) anomaly (mmol/m^3) in the MID-FUTURE of the RCP4.5 scenario in the five layers: 0-50 m, 50-100 m, 100-200 m, 200-500 m and 500-800 m

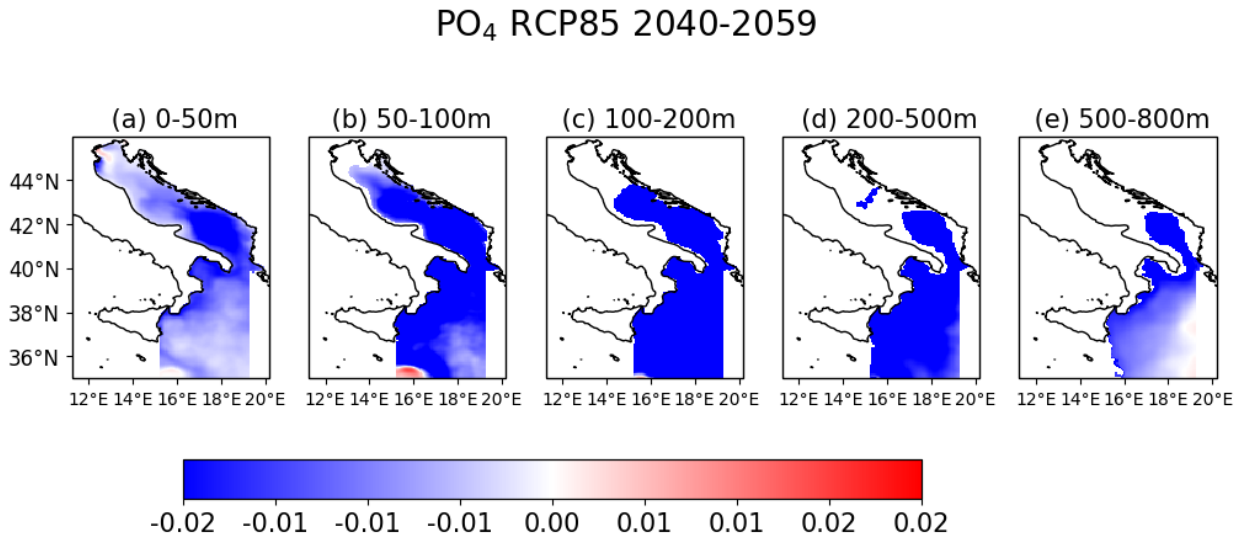

Figure 10 - Mean phosphate (PO_4) anomaly (mmol/m^3) in the MID-FUTURE of the RCP8.5 scenario in the five layers: 0-50 m, 50-100 m, 100-200 m, 200-500 m and 500-800 m

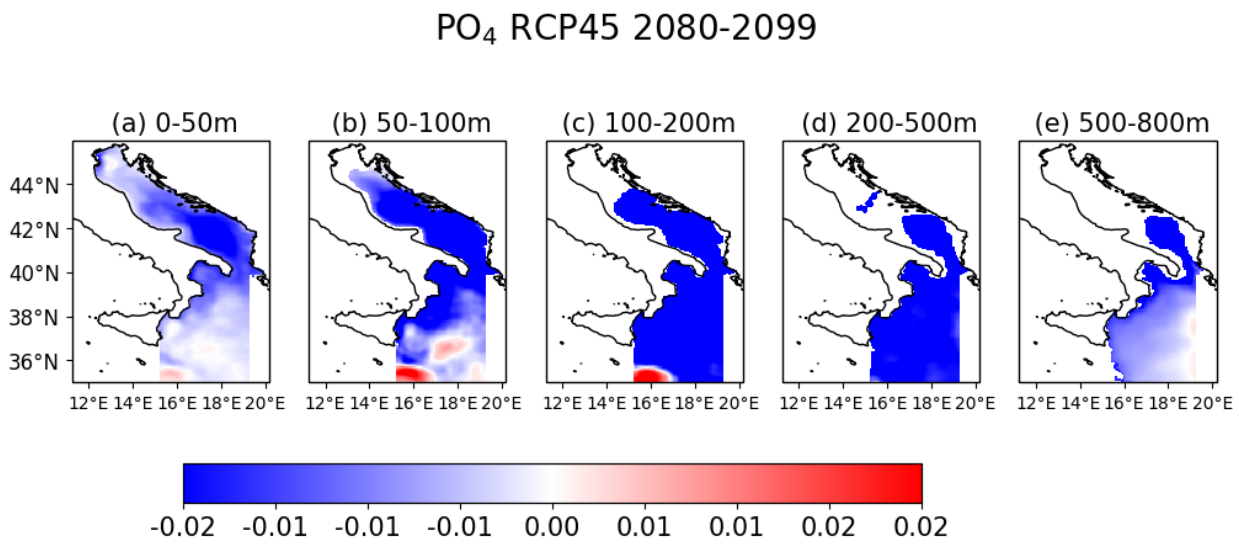

Figure 11 - Mean phosphate (PO_4) anomaly (mmol/m^3) in the FAR-FUTURE of the RCP4.5 scenario in the five layers: 0-50 m, 50-100 m, 100-200 m, 200-500 m and 500-800 m

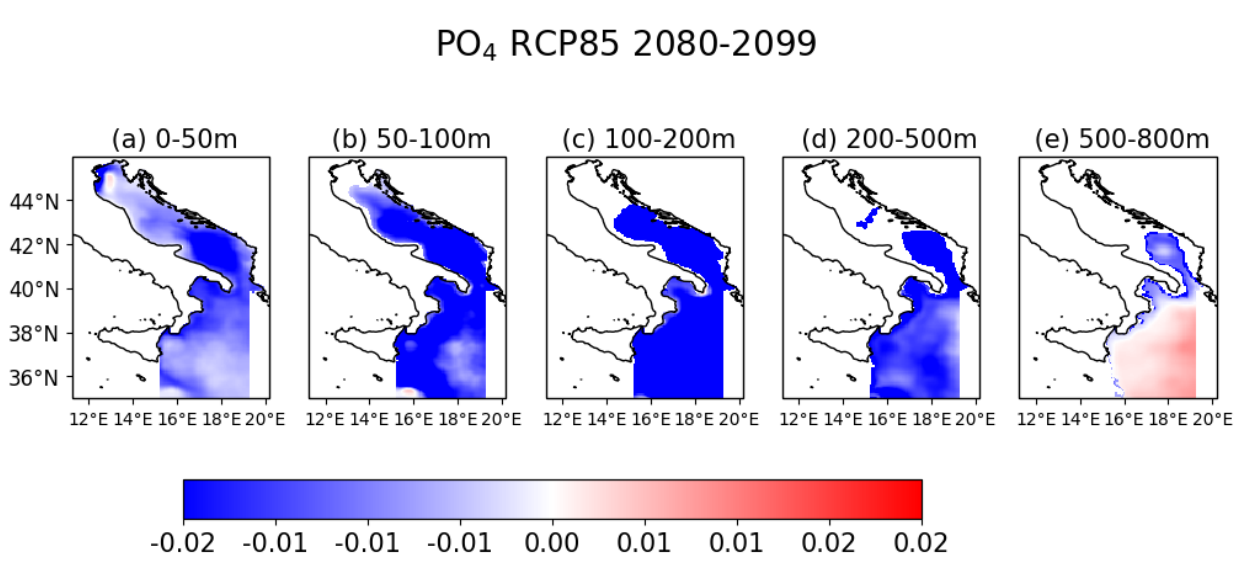

Figure 12 - Mean phosphate (PO_4) anomaly (mmol/m^3) in the FAR-FUTURE of the RCP8.5 scenario in the five layers: 0-50 m, 50-100 m, 100-200 m, 200-500 m and 500-800 m

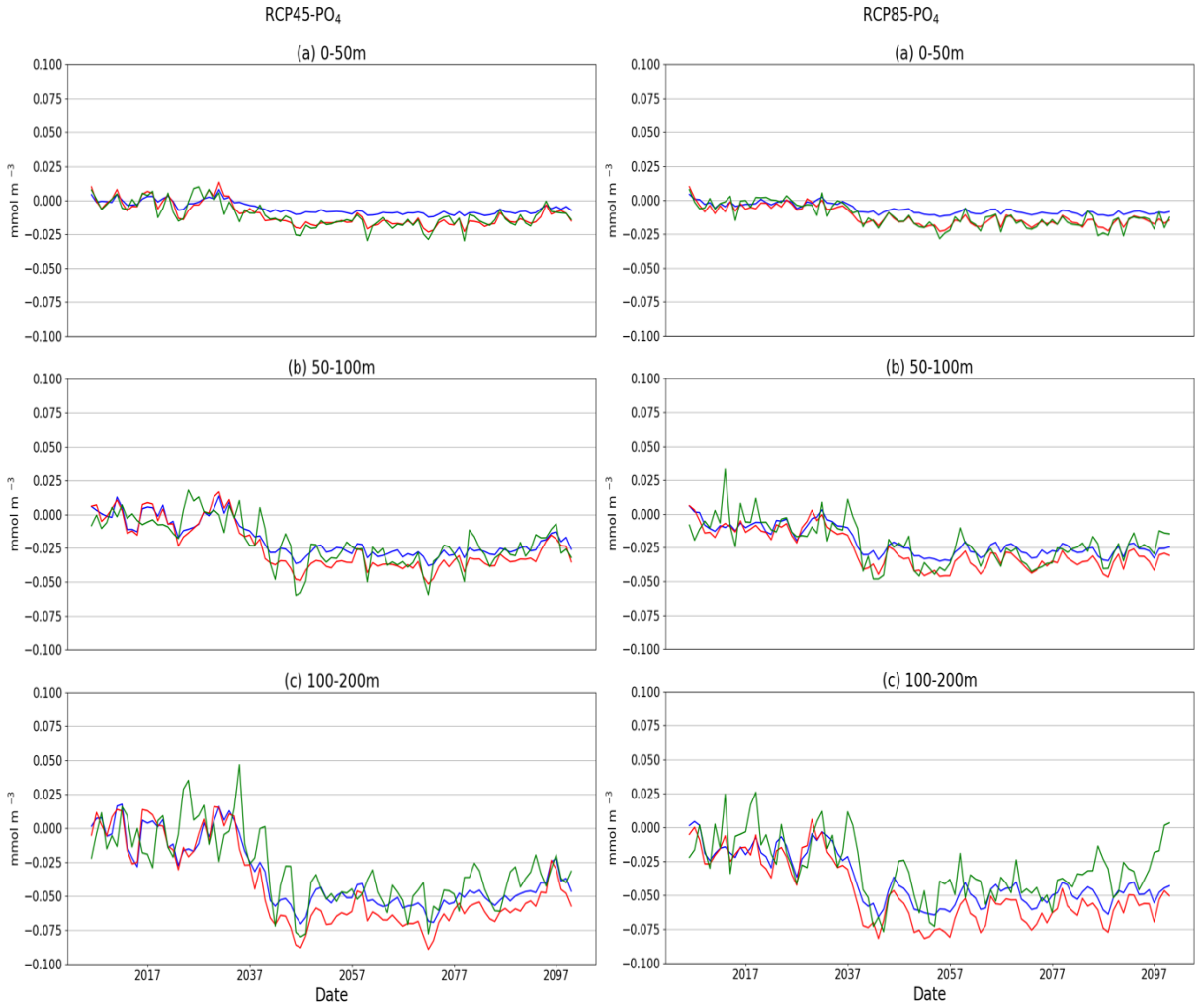

Figure 13 - Annual timeseries of phosphate anomalies (mmol/m^3) in the three inshore (depth less than 200 m) areas of the Adriatic-Ionian Sea: GSA17 - northern Adriatic (blue), GSA18 - southern Adriatic (red) and GSA19 - Ionian (green). Timeseries cover the 2005-2099 period for the two emission RCP4.5 (left) and RCP8.5 (right) scenarios.

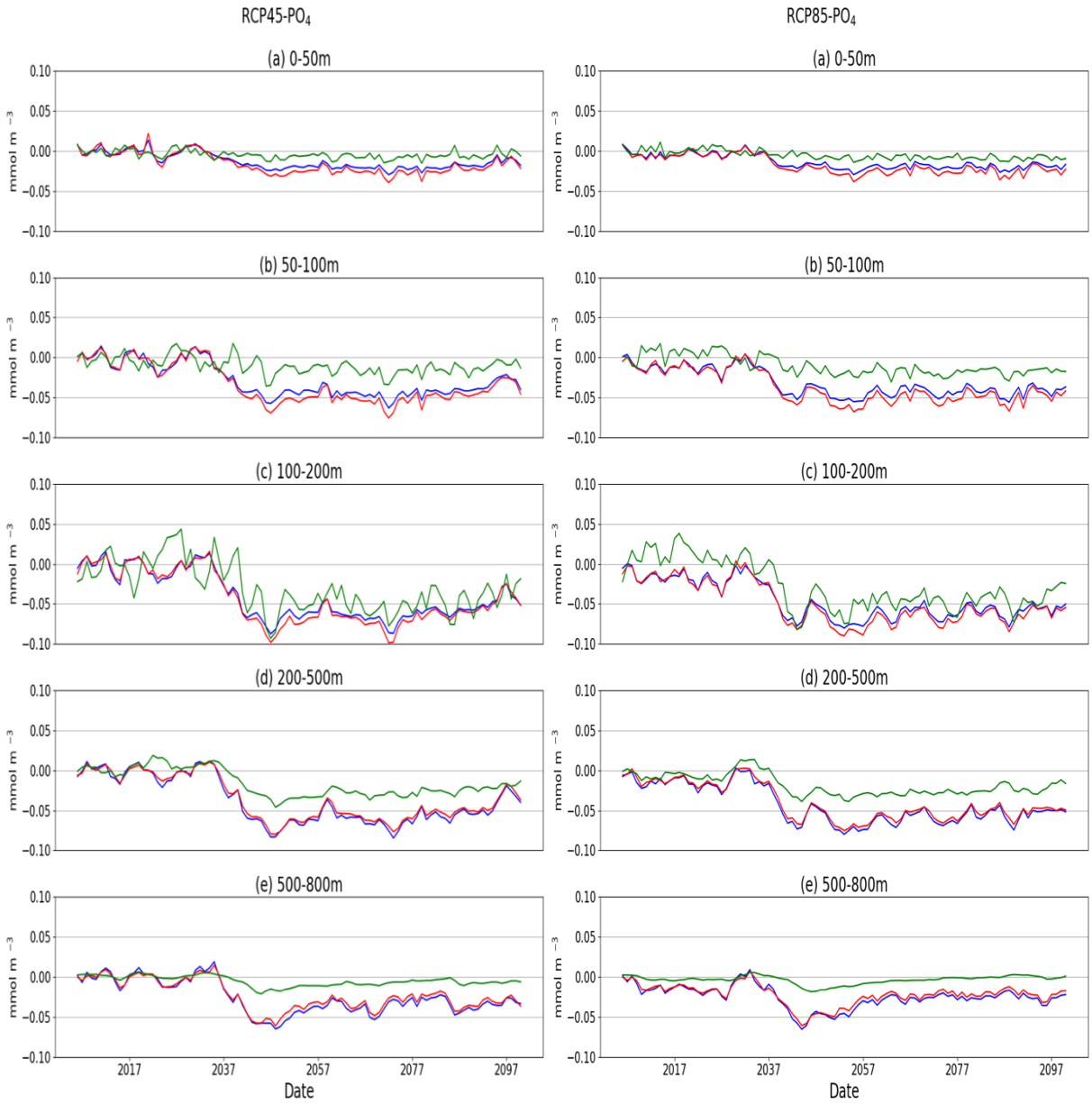

Figure 14 - Annual timeseries of phosphate anomalies (mmol/m^3) in the three offshore (deeper than 200 m) areas of the Adriatic-Ionian Sea: GSA17 - northern Adriatic (blue), GSA18 - southern Adriatic (red) and GSA19 - Ionian (green). Timeseries cover the 2005-2099 period for the two emission RCP4.5 (left) and RCP8.5 (right) scenarios.

Phytoplankton biomass and chlorophyll

The maps of Figures 15-18 and Figures 21-24 shows the anomalies in the two future periods under the emission scenario RCP4.5 and RCP8.5 for the two variables: phytoplankton biomass and chlorophyll, respectively. Given the tight relationship between carbon biomass of phytoplankton and its chlorophyll-a content, the future scenario simulations predict highly correlated anomalies for these two variables. In fact, both variables show a decrease in the concentrations at the surface (0-50 m) and subsurface (50-100 m) in both scenarios and periods. The decrease is due to the increase of the ecosystem metabolism induced by the rise of water temperature (see D 4.1.2). Indeed the increase of losing processes (i.e., respiration and mortality) exceeds the increase of the production processes (Lazzari et al., 2014). Two small spotty areas with positive anomalies at surface are identified in the northernmost part of the Adriatic and south-western part of the GSA 19. An slight increase in the concentration of phytoplankton biomass and chlorophyll-a is also depicted in the 100-200 m layer of the Ionian sea, and it is associated with a change of the location of the deep chlorophyll-a maximum.

The figures 19-20 (phytoplankton carbon biomass) and 25-26 (chlorophyll) show the corresponding anomaly timeseries of three GSA areas in their inshore (Fig. 19 and Fig. 25) and offshore zones (Fig. 20 and Fig. 26). The decreases of phytoplankton biomass and chlorophyll become clearly evident after 2030-2040 (i.e., overcoming the interannual variability) and continue till the end of the century, and it is more marked in the RCP8.5 scenario due to the stronger increase of temperature.

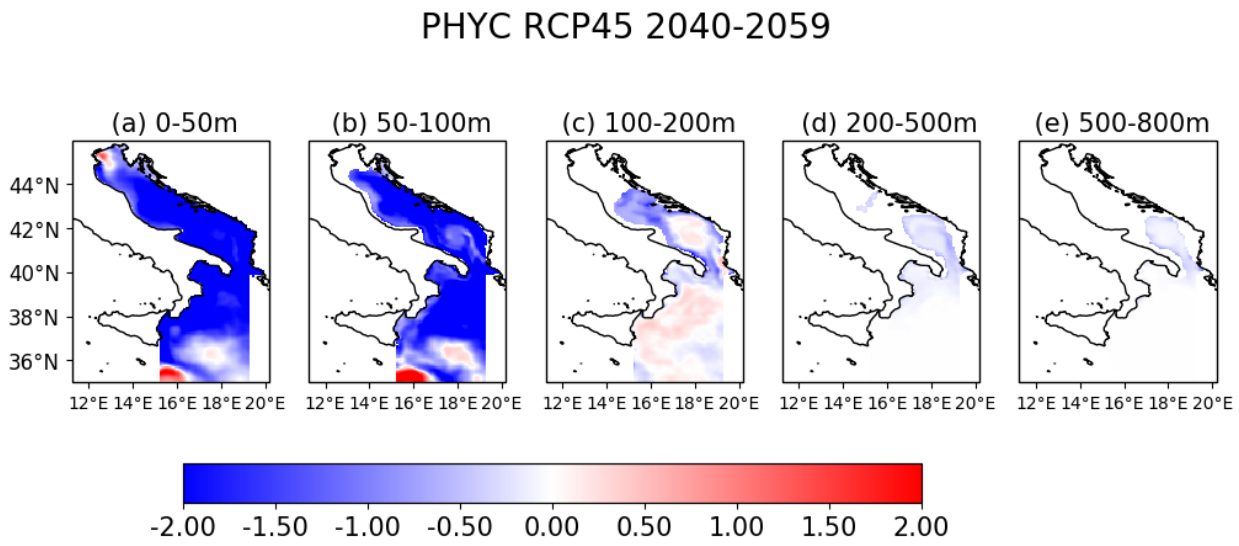

Figure 15 - Mean phytoplankton carbon biomass (PHYC) anomaly (mgC/m^3) in the MID-FUTURE of the RCP4.5 scenario in the five layers: 0-50 m, 50-100 m, 100-200 m, 200-500 m and 500-800 m

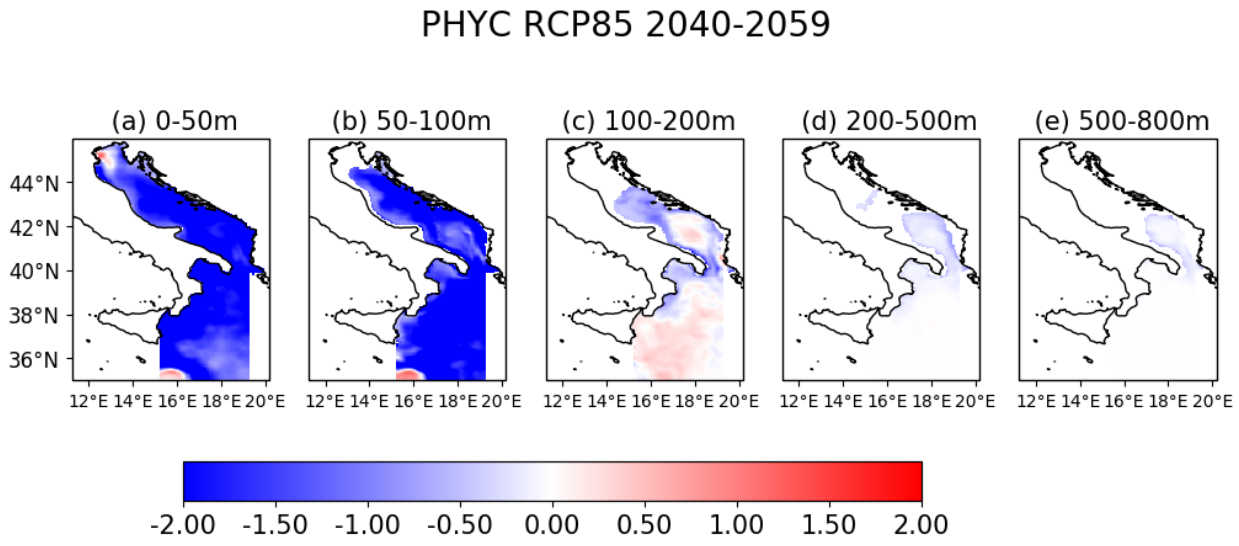

Figure 16 - Mean phytoplankton carbon biomass (PHYC) anomaly (mgC/m^3) in the MID-FUTURE of the RCP8.5 scenario in the five layers: 0-50 m, 50-100 m, 100-200 m, 200-500 m and 500-800 m

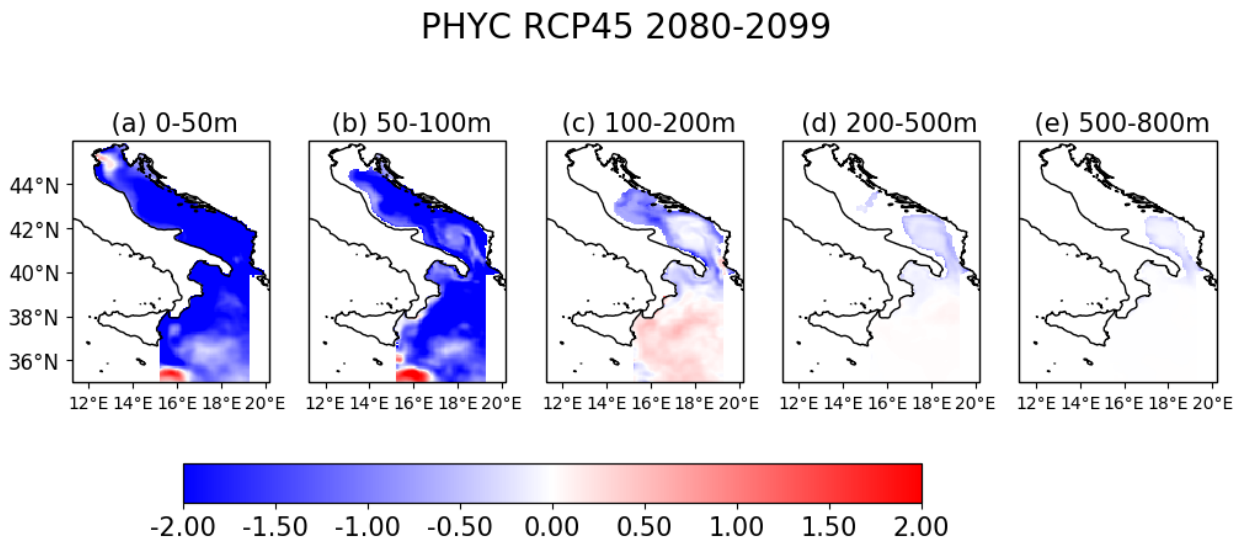

Figure 17 - Mean phytoplankton carbon biomass (PHYC) anomaly (mgC/m^3) in the FAR-FUTURE of the RCP4.5 scenario in the five layers: 0-50 m, 50-100 m, 100-200 m, 200-500 m and 500-800 m

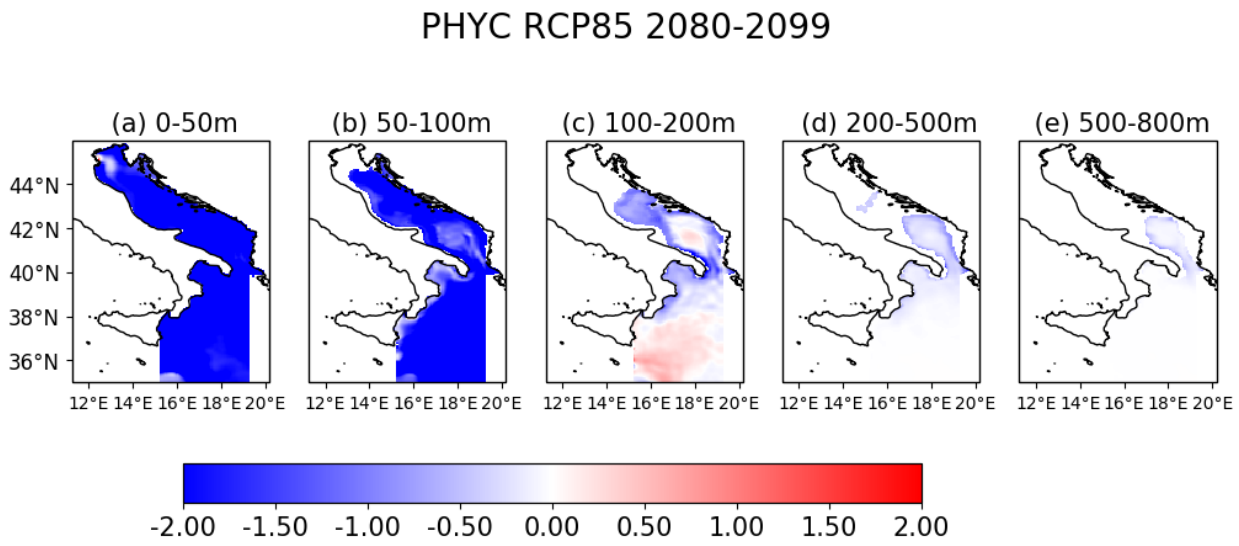

Figure 18 - Mean phytoplankton carbon biomass (PHYC) anomaly (mgC/m^3) in the FAR-FUTURE of the RCP8.5 scenario in the five layers: 0-50 m, 50-100 m, 100-200 m, 200-500 m and 500-800 m

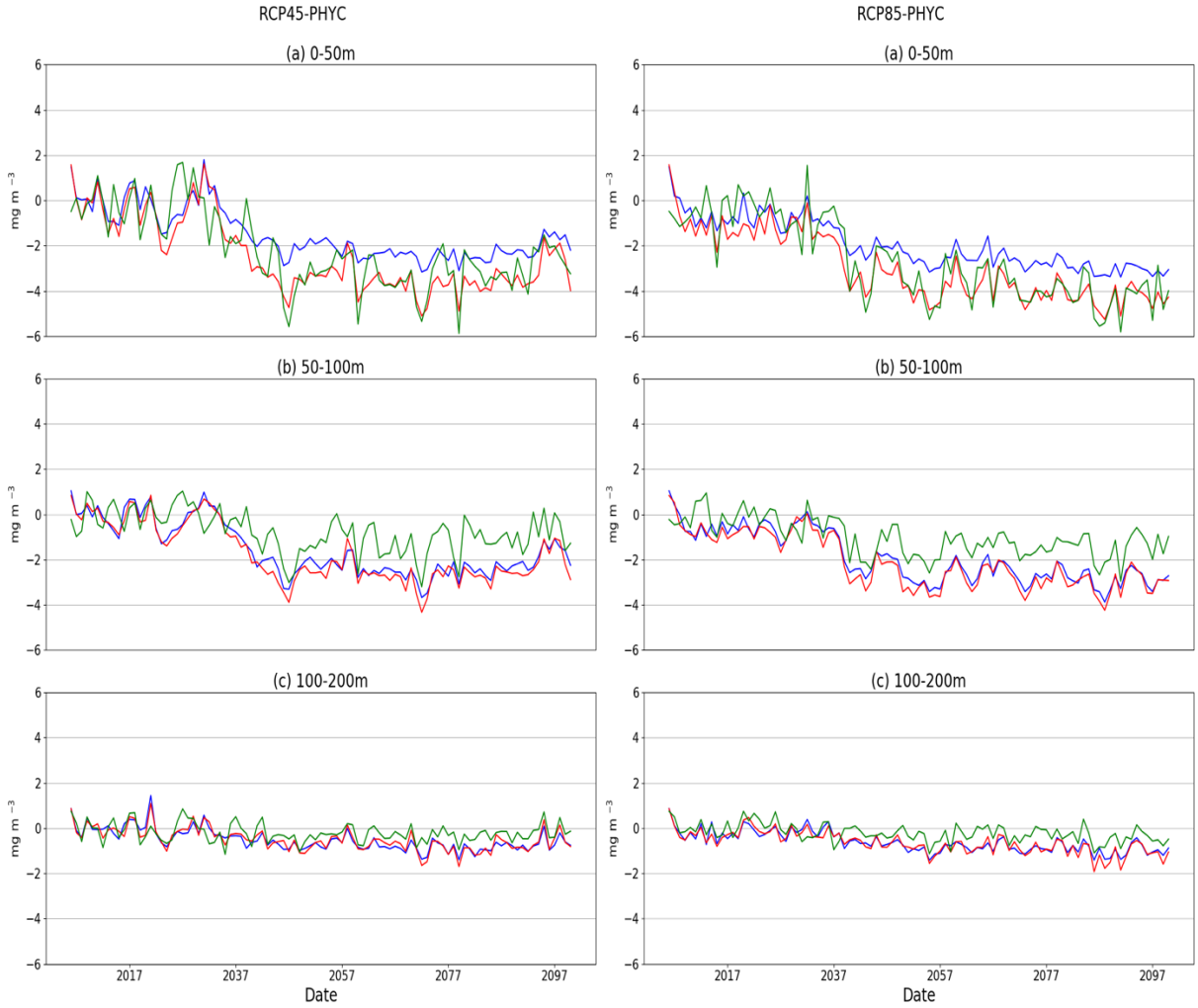

Figure 19 - Annual timeseries of phytoplankton biomass anomalies (mgC/m^3) in the three inshore (depth less than 200 m) areas of the Adriatic-Ionian Sea: GSA17 - northern Adriatic (blue), GSA18 - southern Adriatic (red) and GSA19 - Ionian (green). Timeseries cover the 2005-2099 period for the two emission RCP4.5 (left) and RCP8.5 (right) scenarios.

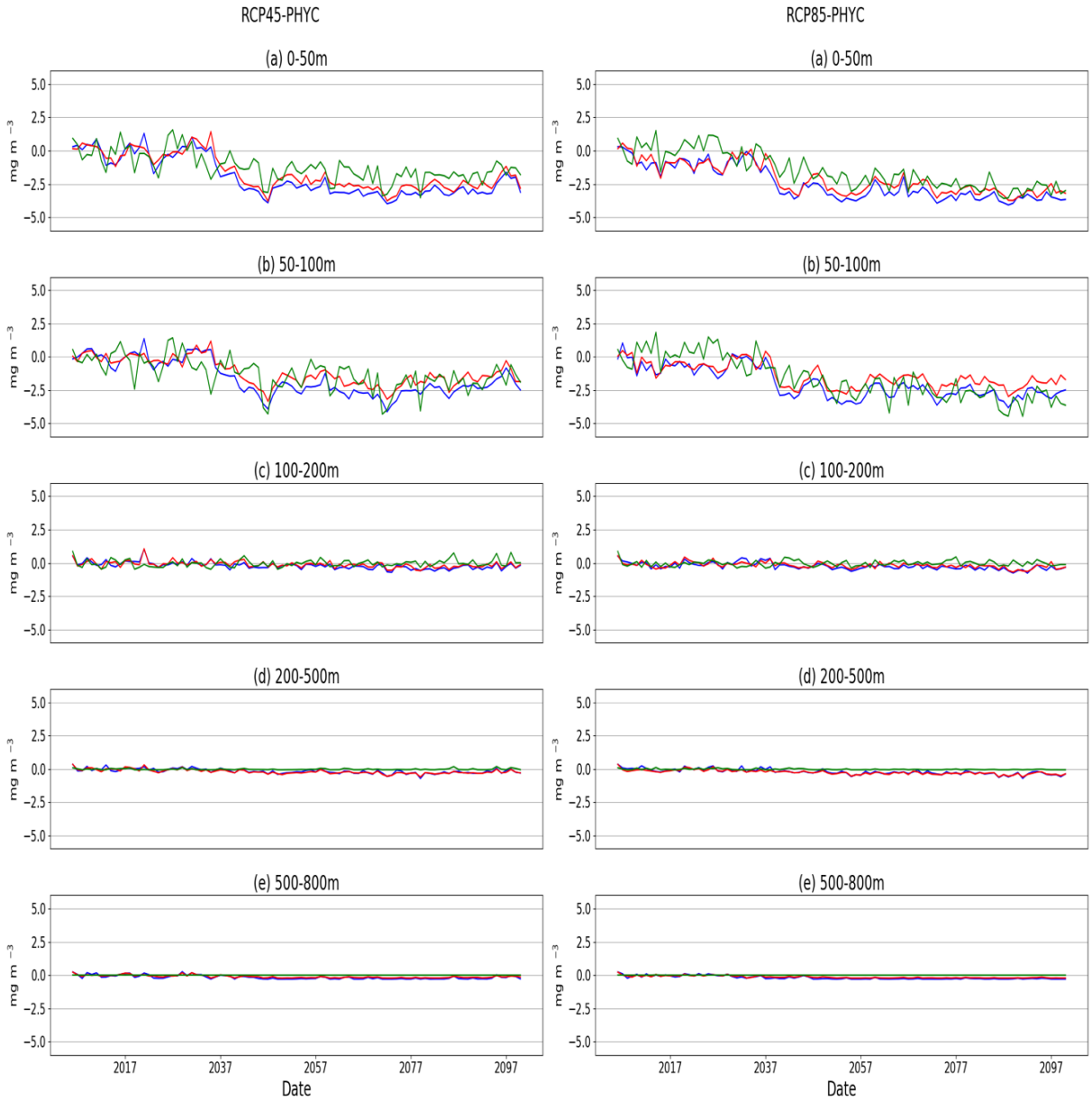

Figure 20 - Annual timeseries of phytoplankton biomass anomalies (mgC/m^3) in the three offshore (deeper than 200 m) areas of the Adriatic-Ionian Sea: GSA17 - northern Adriatic (blue), GSA18 - southern Adriatic (red) and GSA19 - Ionian (green). Timeseries cover the 2005-2099 period for the two emission RCP4.5 (left) and RCP8.5 (right) scenarios.

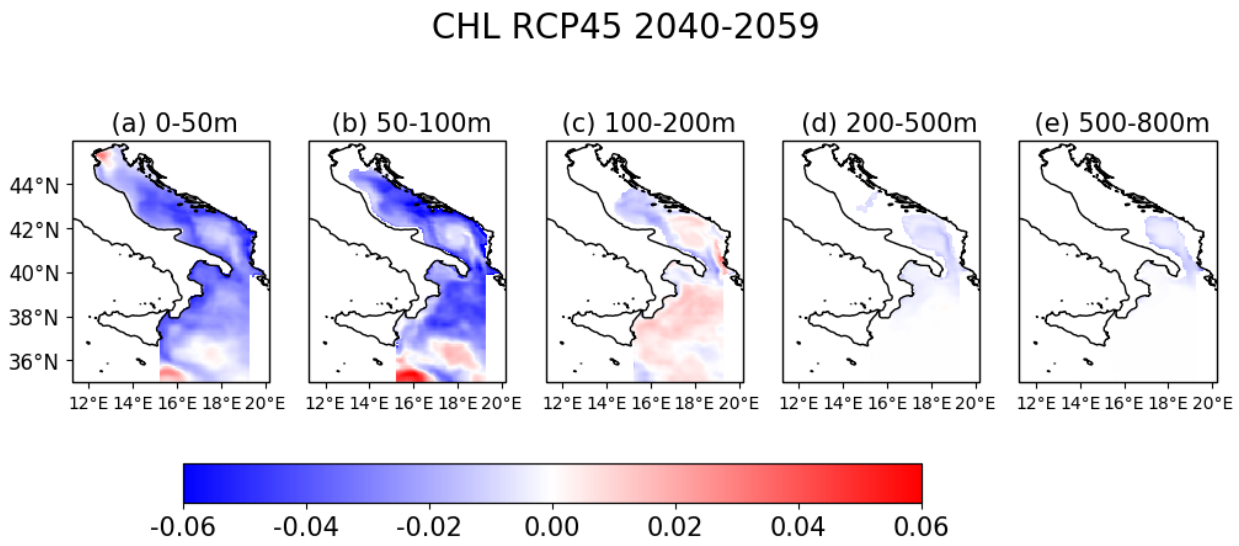

Figure 21- Mean chlorophyll (CHL) anomaly (mgC/m^3) in the MID-FUTURE of the RCP4.5 scenario in the five layers: 0-50 m, 50-100 m, 100-200 m, 200-500 m and 500-800 m

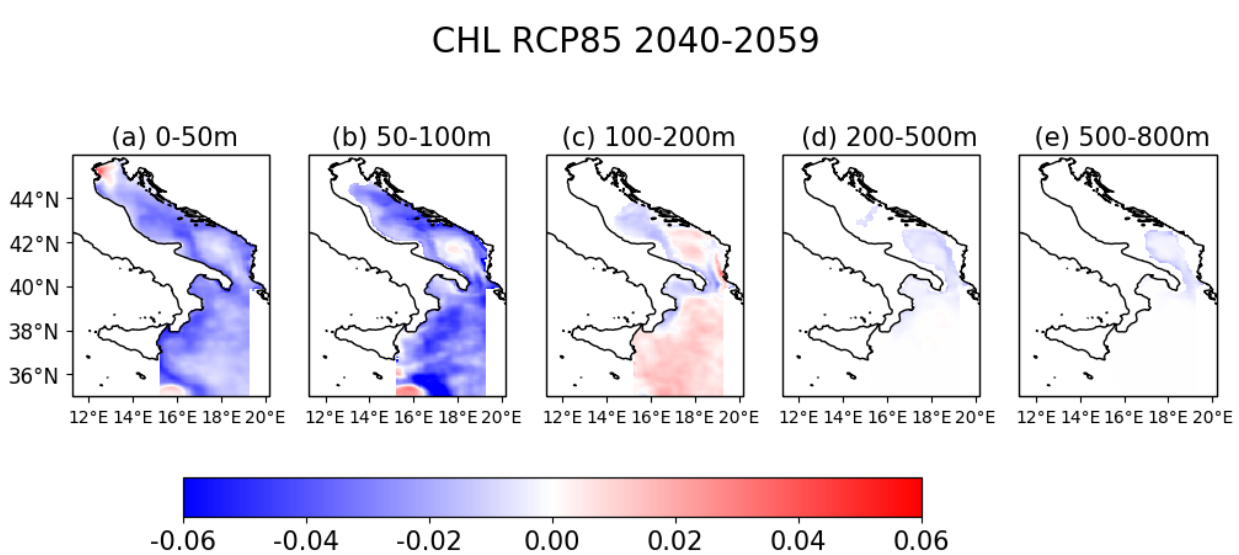

Figure 22 - Mean chlorophyll (CHL) anomaly (mgC/m^3) in the MID-FUTURE of the RCP8.5 scenario in the five layers: 0-50 m, 50-100 m, 100-200 m, 200-500 m and 500-800 m

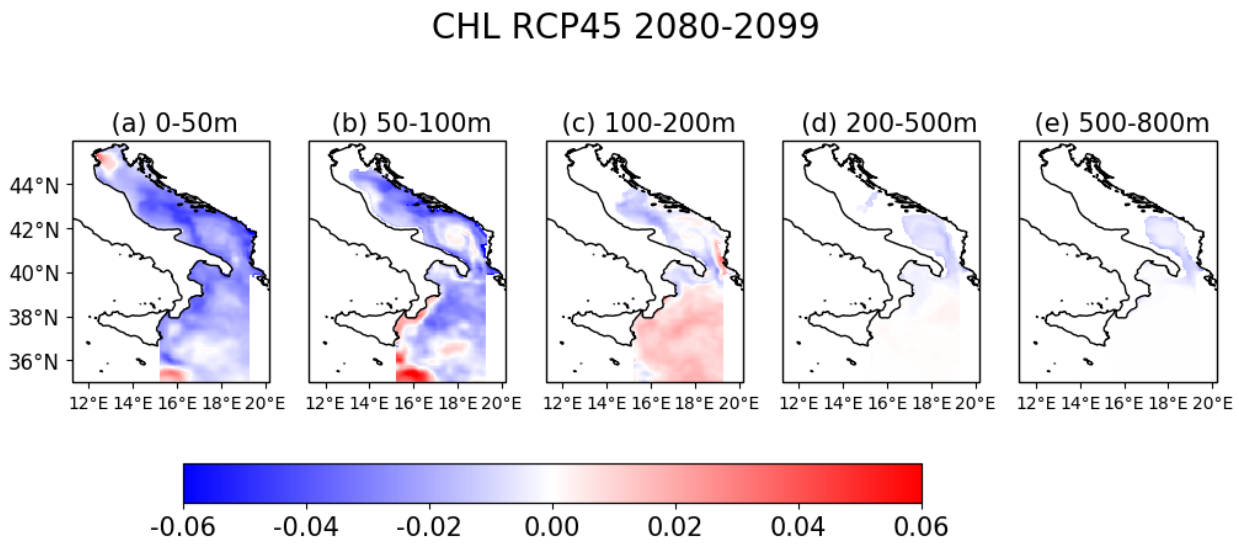

Figure 23 - Mean chlorophyll (CHL) anomaly (mgC/m^3) in the FAR-FUTURE of the RCP4.5 scenario in the five layers: 0-50 m, 50-100 m, 100-200 m, 200-500 m and 500-800 m

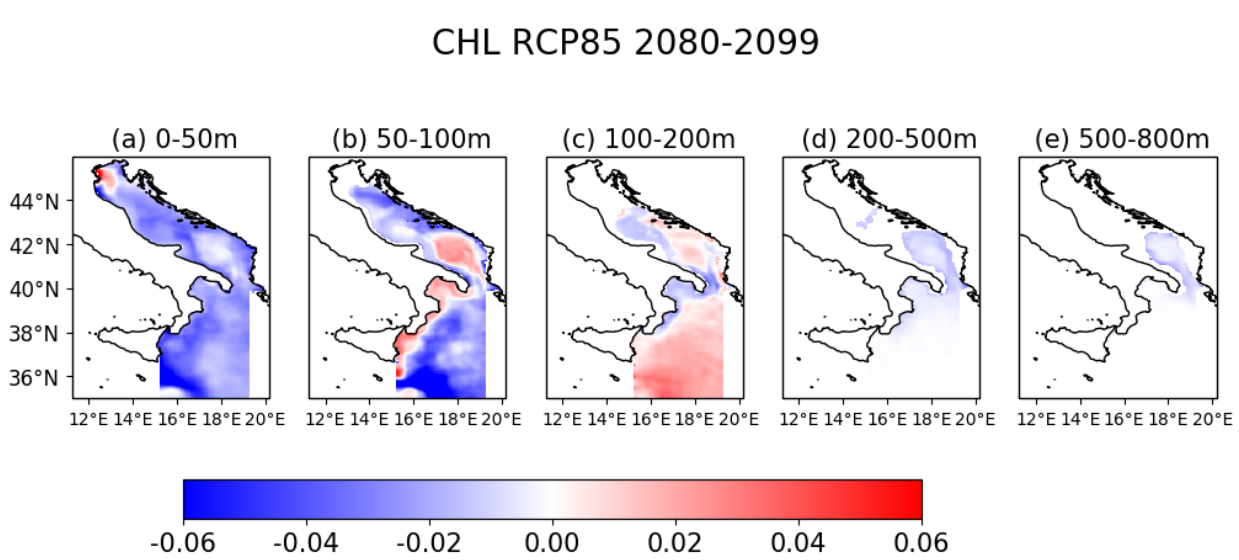

Figure 24 - Mean chlorophyll (CHL) anomaly (mgC/m^3) in the FAR-FUTURE of the RCP8.5 scenario in the five layers: 0-50 m, 50-100 m, 100-200 m, 200-500 m and 500-800 m

Figure 25 - Annual timeseries of Chlorophyll-a concentration anomalies (mgChl-a/m^3) in the three inshore (depth less than 200 m) areas of the Adriatic-Ionian Sea: GSA17 - northern Adriatic (blue), GSA18 - southern Adriatic (red) and GSA19 - Ionian (green). Timeseries cover the 2005-2099 period for the two emission RCP4.5 (left) and RCP8.5 (right) scenarios.

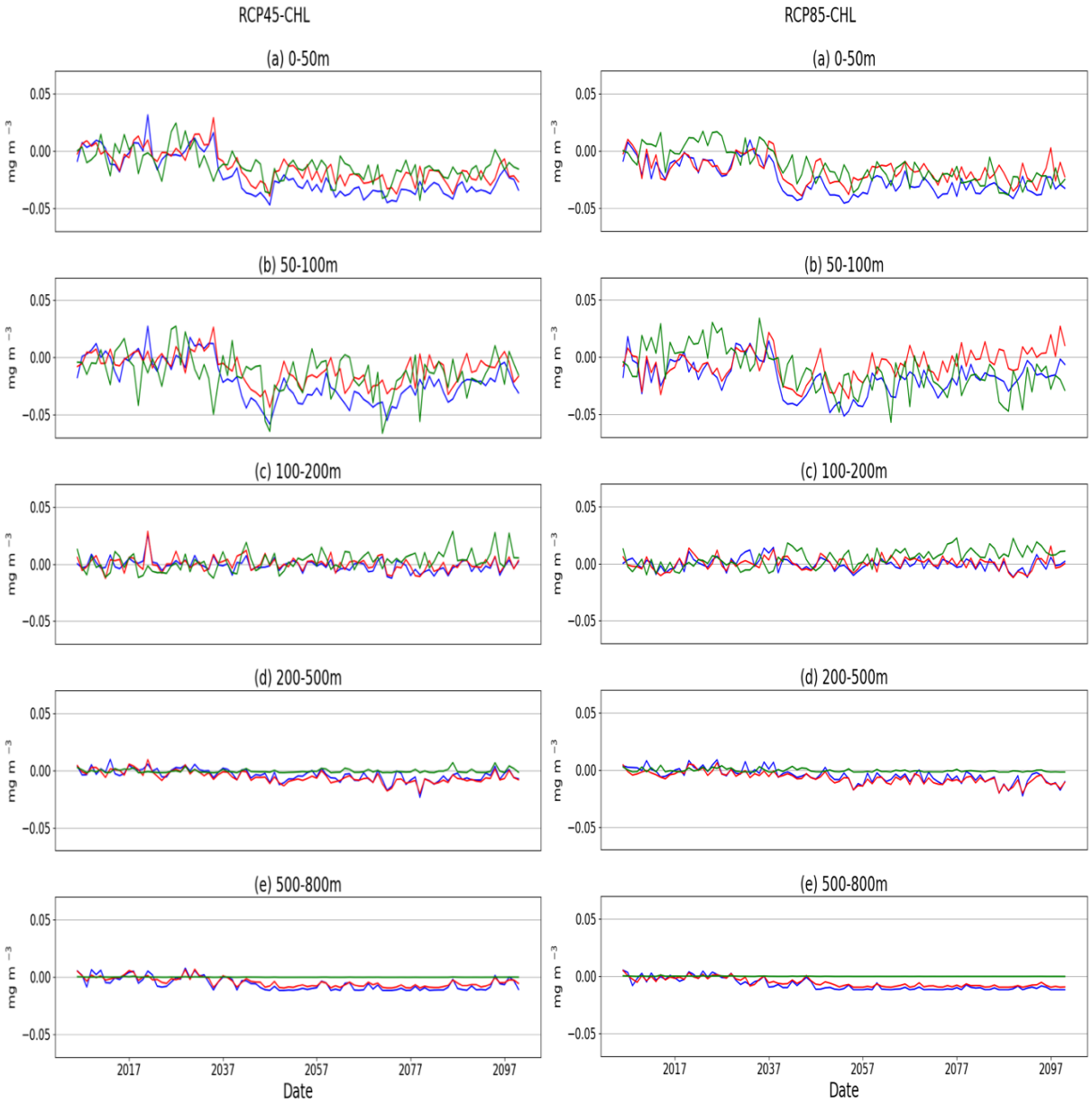

Figure 26 - Annual timeseries of Chlorophyll-a concentration anomalies (mgChl-a/m^3) in the three offshore (deeper than 200 m) areas of the Adriatic-Ionian Sea: GSA17 - northern Adriatic (blue), GSA18 - southern Adriatic (red) and GSA19 - Ionian (green). Timeseries cover the 2005-2099 period for the two emission RCP4.5 (left) and RCP8.5 (right) scenarios.

Primary production

Net primary production (NPP) anomalies computed for the MID-FUTURE and FAR-FUTURE under the two emission scenarios are shown in the maps of Figs. 27-30. NPP is the difference between the carbon fixed during the photosynthesis and the one consumed during the respiration. As reported in the present-day report (D 4.2.1), the mean annual values of NPP at surface are around 7-10 mg/m^3/day in the off-shore areas and up to 20-30 mg/m^3/day in the inshore areas. Then, the productivity values decay rapidly to 0 in the subsurface layer because of the light limitation.

At the surface (0-50 m) layer, the MID-FUTURE shows a quite small negative anomaly of around 0.25-0.5 mg/m^3/day with respect to the present-day condition in both scenarios, whereas the FAR-FUTURE reports an almost balanced condition (i.e., slight negative anomaly in the Adriatic Sea and slight positive anomaly in the Ionian Sea) in the RCP4.5 scenario and a positive anomaly all over the three GSA areas in the RCP 8.5 scenario. Small-size spots of positive anomalies are visible in the coastal areas of the northern Adriatic Sea in both scenarios and they are associated with the positive anomaly of nutrients.

The increase of the RCP8.5 scenario is associated with the projected increase of temperature (D 4.1.2). It is worth to remind that the increase of temperature influences (i.e., by increasing) other loss terms rate (e.g., mortality, community respiration) which over-counterbalances the increase of the primary production and produces the negative anomaly of biomass at the end of the century.

The plots of the timeseries (Figs. 31-32) show that the general increase of NPP at surface occurs mainly during the second half of the 21st century, whereas the initial decrease seems associated with the negative anomalies of the nutrient concentrations observed around the 2030s.

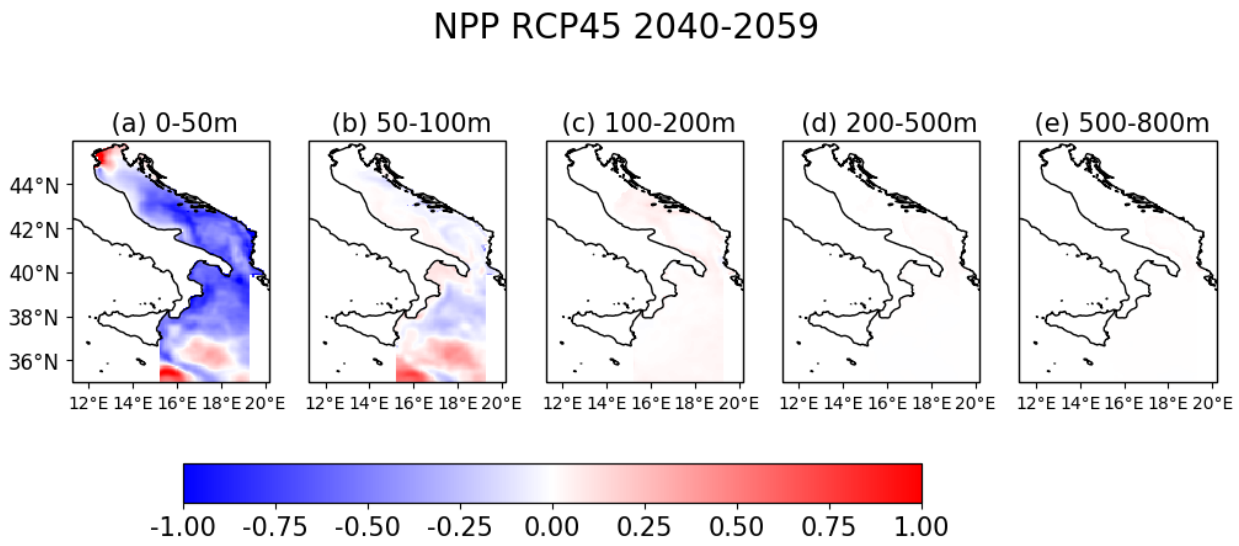

Figure 27 - Mean net primary production (NPP) anomalies (mgC/m^3/day) in the MID-FUTURE of the RCP4.5 scenario in the five layers: 0-50 m, 50-100 m, 100-200 m, 200-500 m and 500-800 m

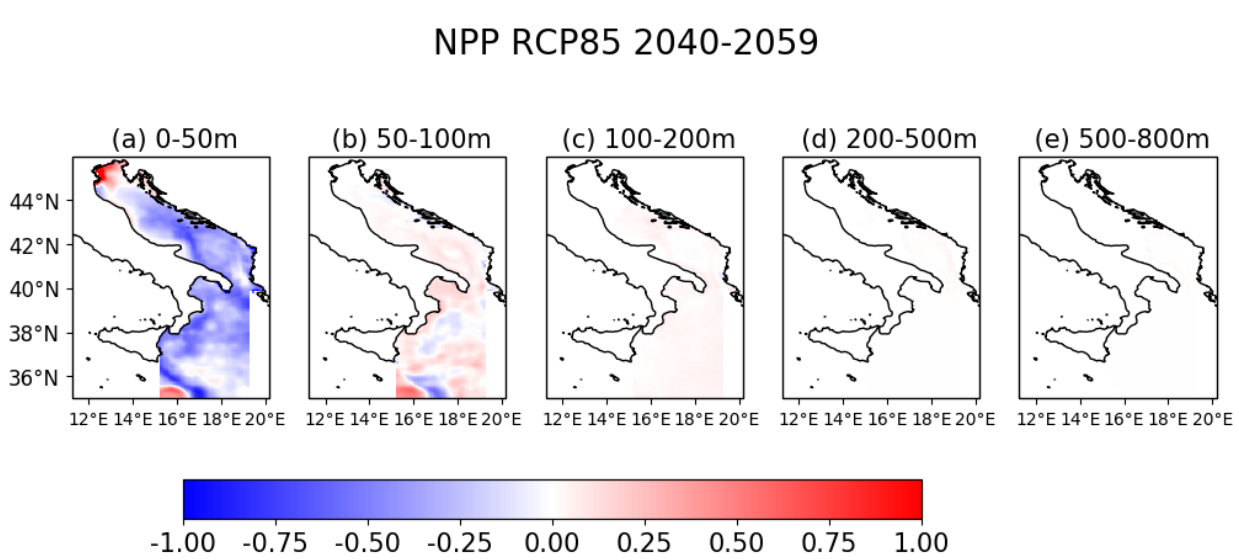

Figure 28 - Mean net primary production (NPP) anomalies (mgC/m^3/day) in the MID-FUTURE of the RCP8.5 scenario in the five layers: 0-50 m, 50-100 m, 100-200 m, 200-500 m and 500-800 m

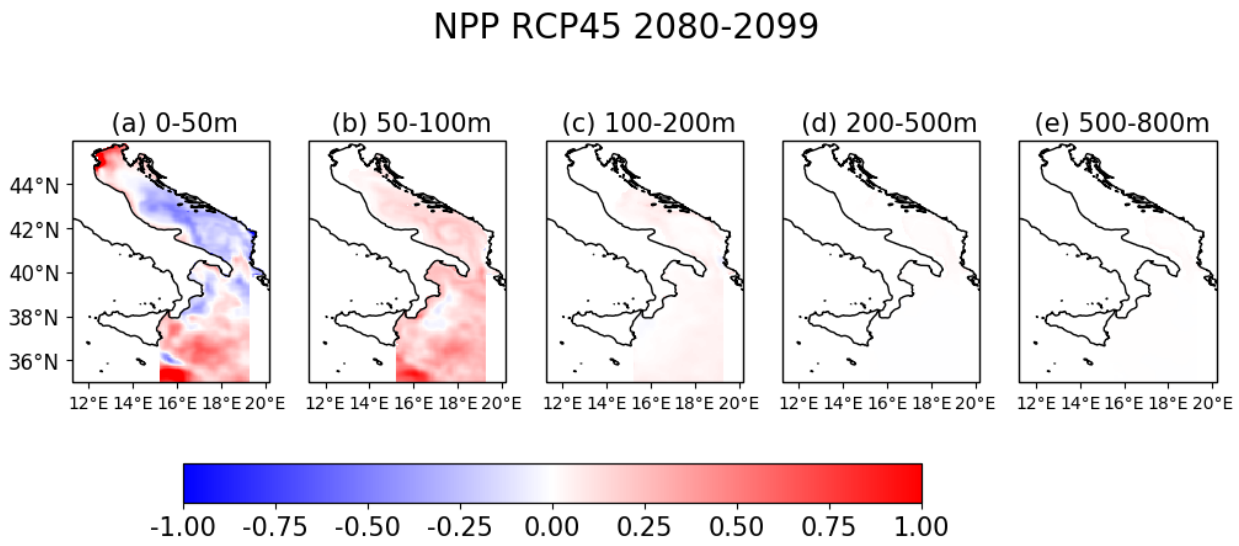

Figure 29 - Mean net primary production (NPP) anomalies (mgC/m^3/day) in the FAR-FUTURE of the RCP4.5 scenario in the five layers: 0-50 m, 50-100 m, 100-200 m, 200-500 m and 500-800 m

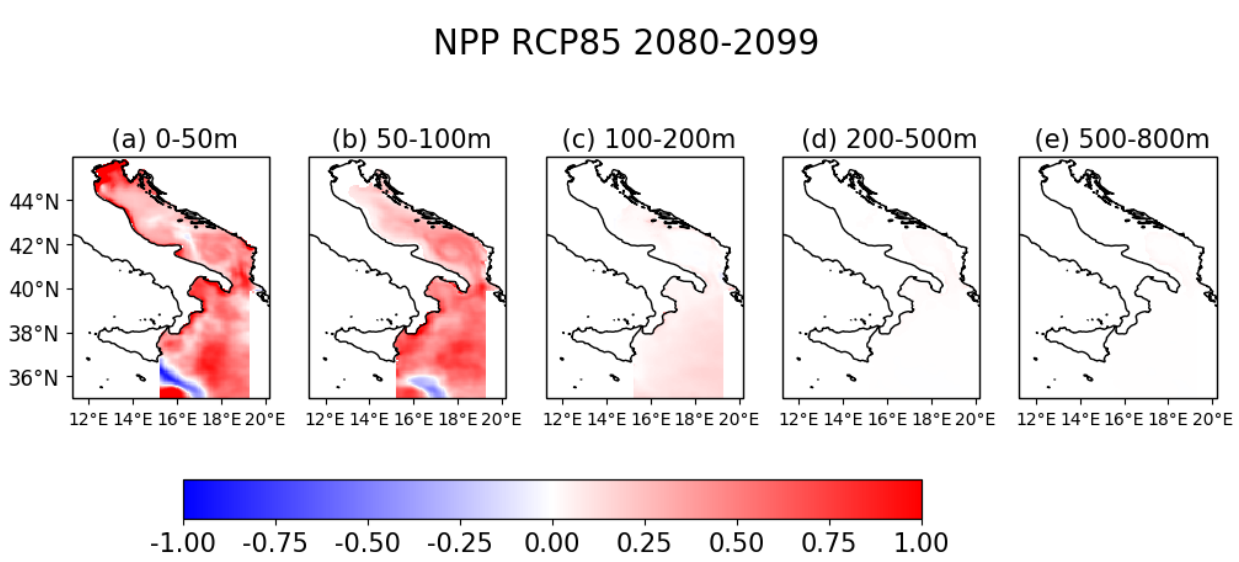

Figure 30 - Mean net primary production (NPP) anomalies (mgC/m^3/day) in the FAR-FUTURE of the RCP8.5 scenario in the five layers: 0-50 m, 50-100 m, 100-200 m, 200-500 m and 500-800 m

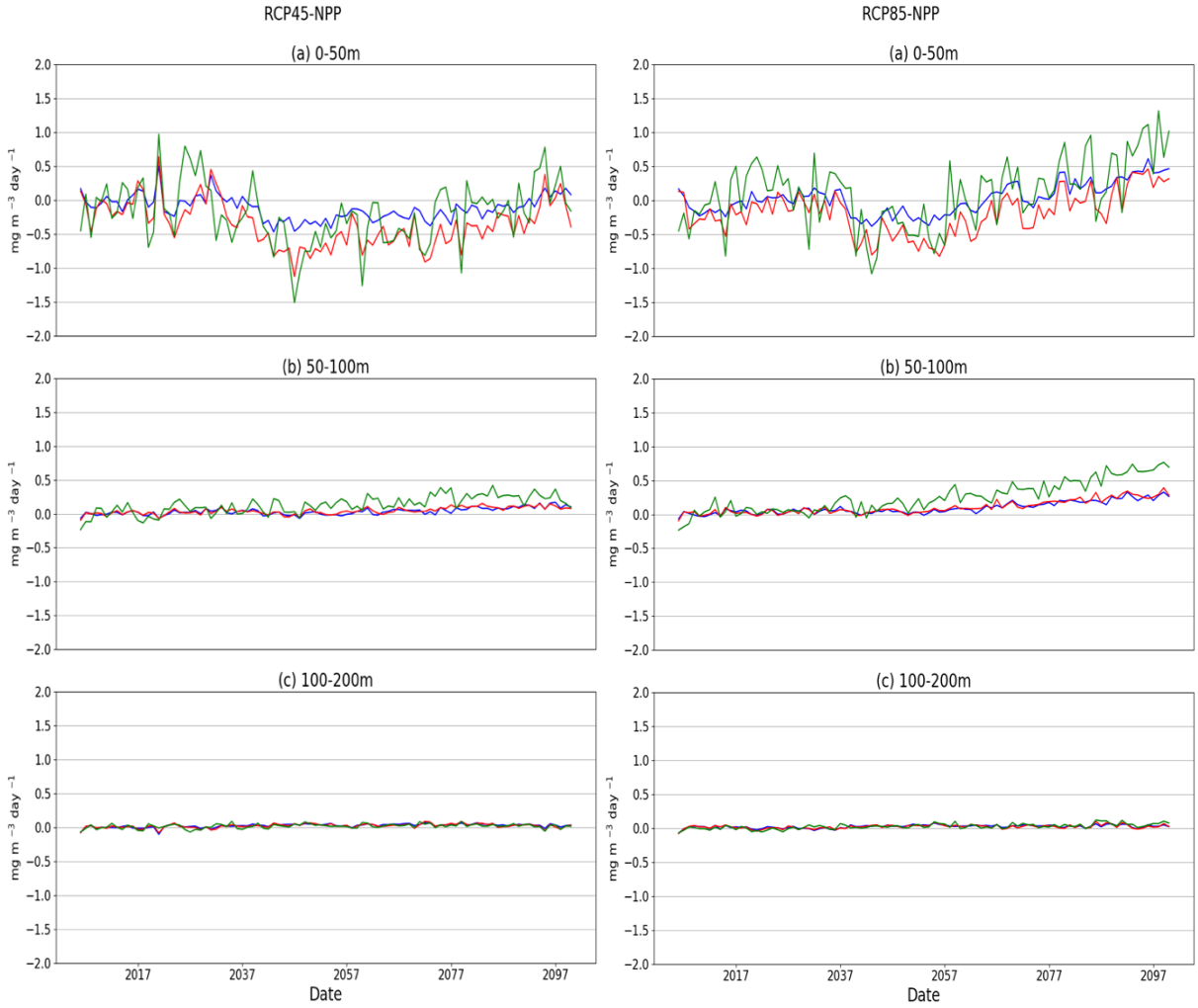

Figure 31 - Annual timeseries of net primary production (NPP) anomalies (mgC/m^3/day) in the three inshore (depth less than 200 m) areas of the Adriatic-Ionian Sea: GSA17 - northern Adriatic (blue), GSA18 - southern Adriatic (red) and GSA19 - Ionian (green). Timeseries cover the 2005-2099 period for the two emission RCP4.5 (left) and RCP8.5 (right) scenarios.

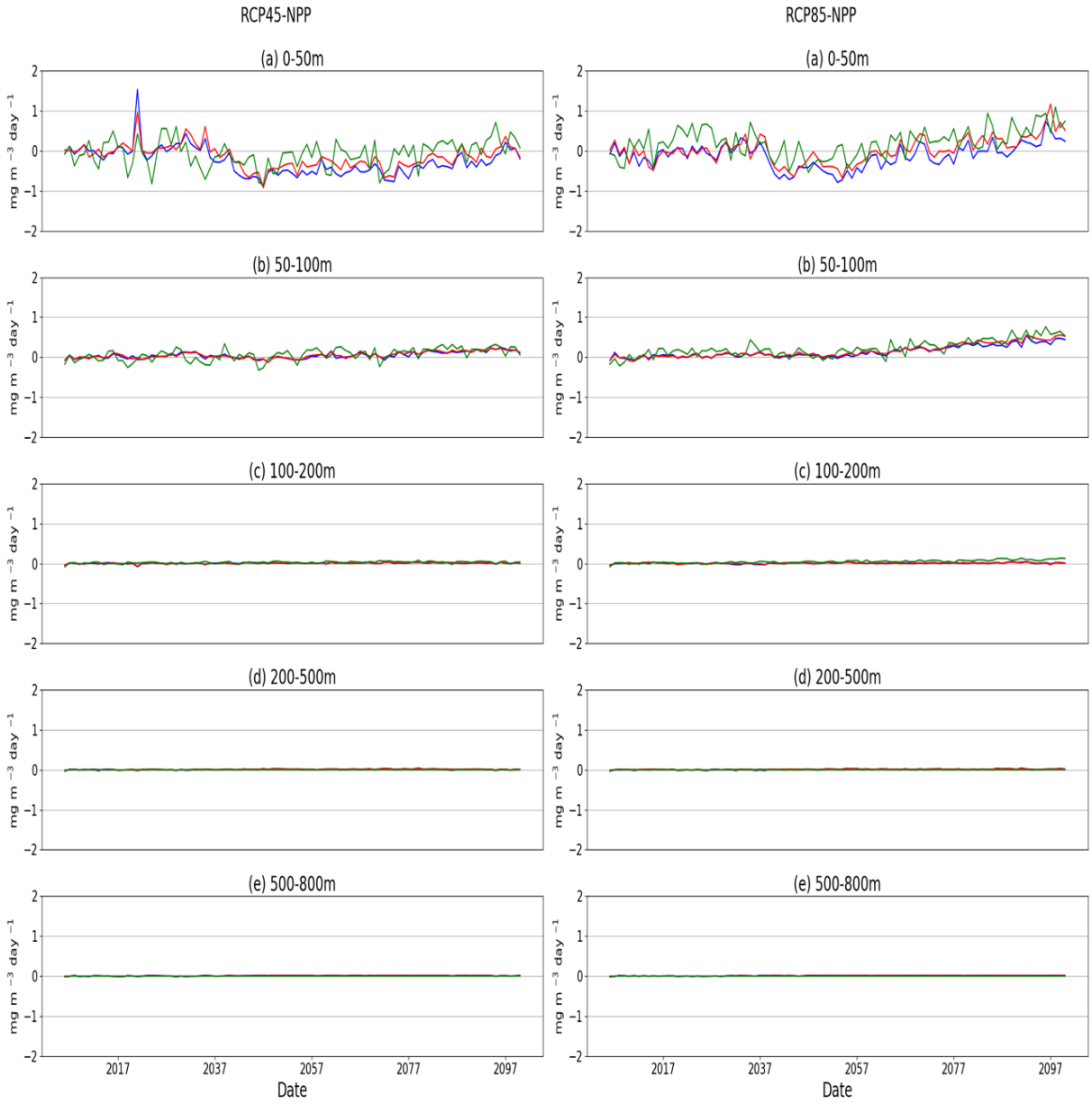

Figure 32 - Annual timeseries of net primary production (NPP) anomalies (mgC/m^3/day) in the three offshore (deeper than 200 m) areas of the Adriatic-Ionian Sea: GSA17 - northern Adriatic (blue), GSA18 - southern Adriatic (red) and GSA19 - Ionian (green). Timeseries cover the 2005-2099 period for the two emission RCP4.5 (left) and RCP8.5 (right) scenarios.

Dissolved oxygen and bottom oxygen

The maps of anomaly of dissolved oxygen (Figs. 33-36) show the presence of a negative decrease at the surface during the 21st century, stronger in RCP8.5 than in RCP4.5. By the end of the century the anomaly can be down to -5/-10 mmol/m^3 in the worst of the two scenarios. On the other hand, while there is a small increase of the oxygen concentration in the intermediate layer associated with an increase of phytoplankton biomass concentration in the MID-FUTURE, the decrease of concentration will affect the entire water column down to 800 m in the FAR-FUTURE.

Figs. 37-38 show the corresponding time series of the three GSA areas in their inshore (Figs. 37) and offshore zones (Fig. 38). The plots show that the trend is monotonic during the entire 21st century and that the decrease of dissolved oxygen affects mainly the surface of the two basins and mainly the inshore areas (Fig. 37). The negative trend is associated with the decrease of oxygen solubility as a response to the increase in the seawater temperature.

Considering the oxygen concentration at the bottom of the water column in the MID-FUTURE (Figs. 39-40) and FAR-FUTURE (Figs 41-42), most of the Adriatic and Ionian will be interested by a general decrease (e.g., negative anomaly values down to -10/-15 mmol/m^3 in the worst-case scenario) which is mainly due to the combination of the decrease of solubility at surface and the reduction of ventilation of the bottom water masses. The southern Adriatic pit appears one of the most negatively impacted areas. A slight positive anomaly (i.e., values of 1-2 mmol/m^3) is instead foreseen in the deepest part of the GSA19 (Ionian Sea) in the FAR-FUTURE of the RCP 4.5 scenario as a response to water mass spatial redistribution (i.e., deep levantine water).

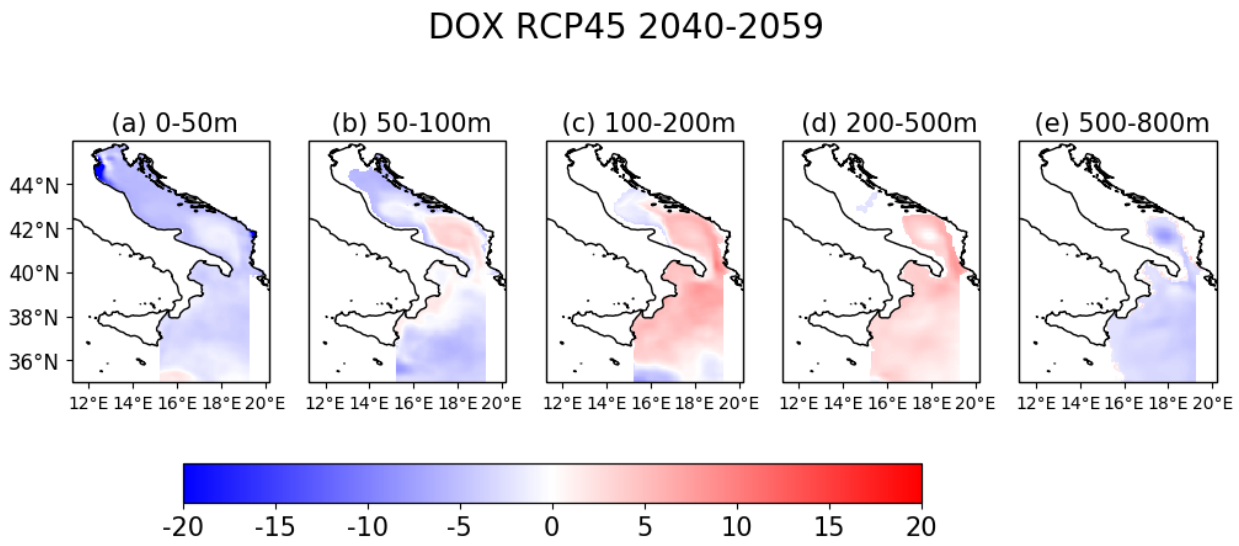

Figure 33 - Mean dissolved oxygen (DOX) anomalies (mmol/m^3) in the MID-FUTURE of the RCP4.5 scenario in the five layers: 0-50 m, 50-100 m, 100-200 m, 200-500 m and 500-800 m

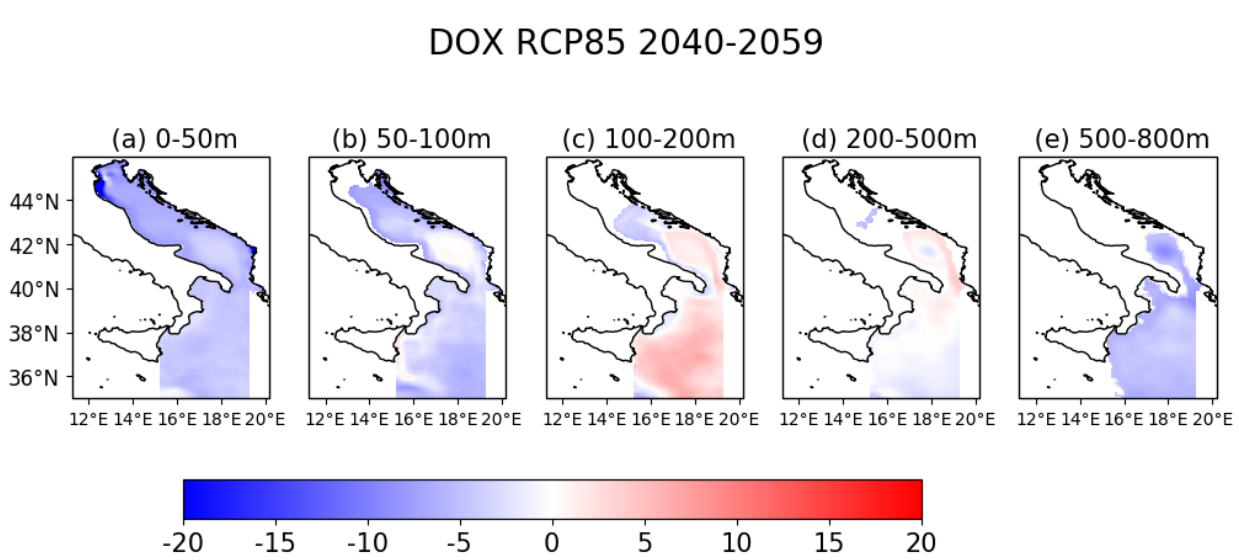

Figure 34 - Mean dissolved oxygen (DOX) anomalies (mmol/m^3) in the MID-FUTURE of the RCP8.5 scenario in the five layers: 0-50 m, 50-100 m, 100-200 m, 200-500 m and 500-800 m

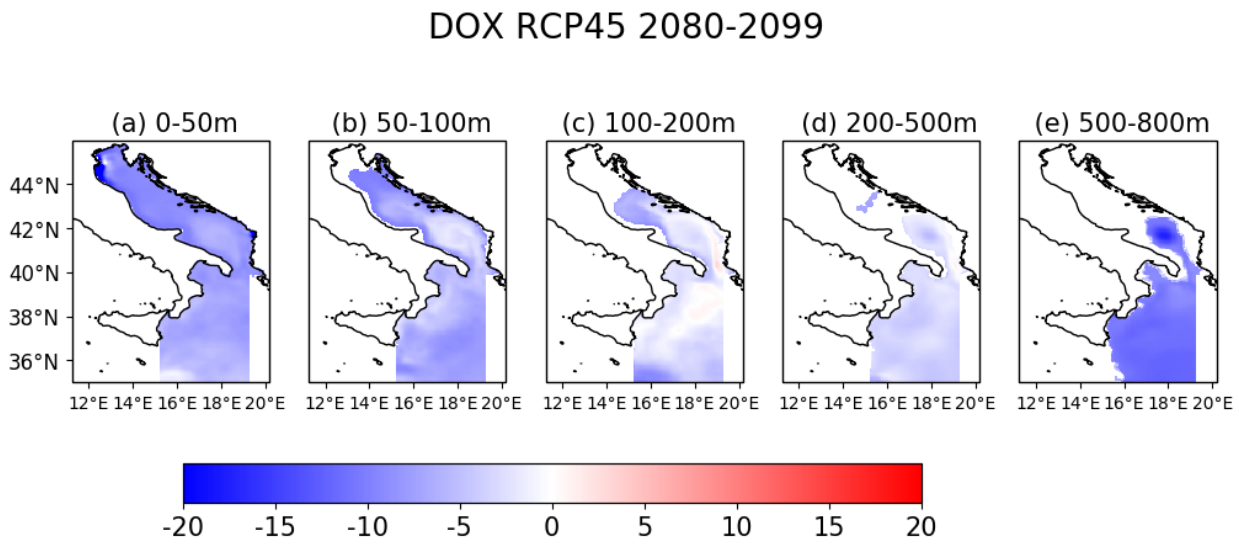

Figure 35 - Mean dissolved oxygen (DOX) anomalies (mmol/m^3) in the FAR-FUTURE of the RCP4.5 scenario in the five layers: 0-50 m, 50-100 m, 100-200 m, 200-500 m and 500-800 m

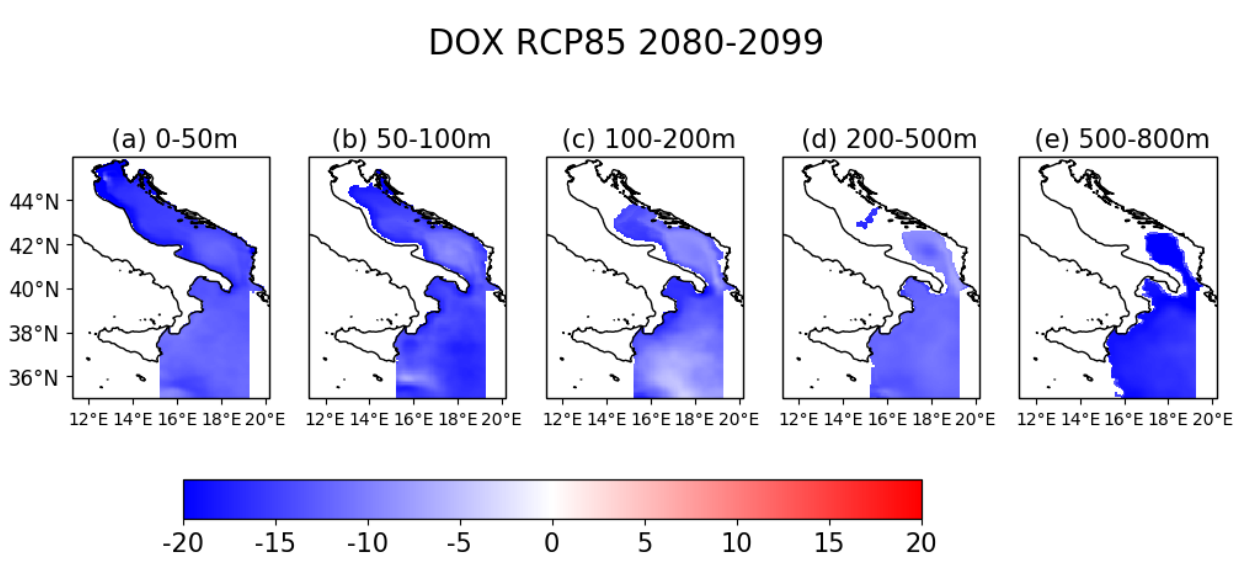

Figure 36 - Mean dissolved oxygen (DOX) anomalies (mmol/m^3) in the FAR-FUTURE of the RCP8.5 scenario in the five layers: 0-50 m, 50-100 m, 100-200 m, 200-500 m and 500-800 m

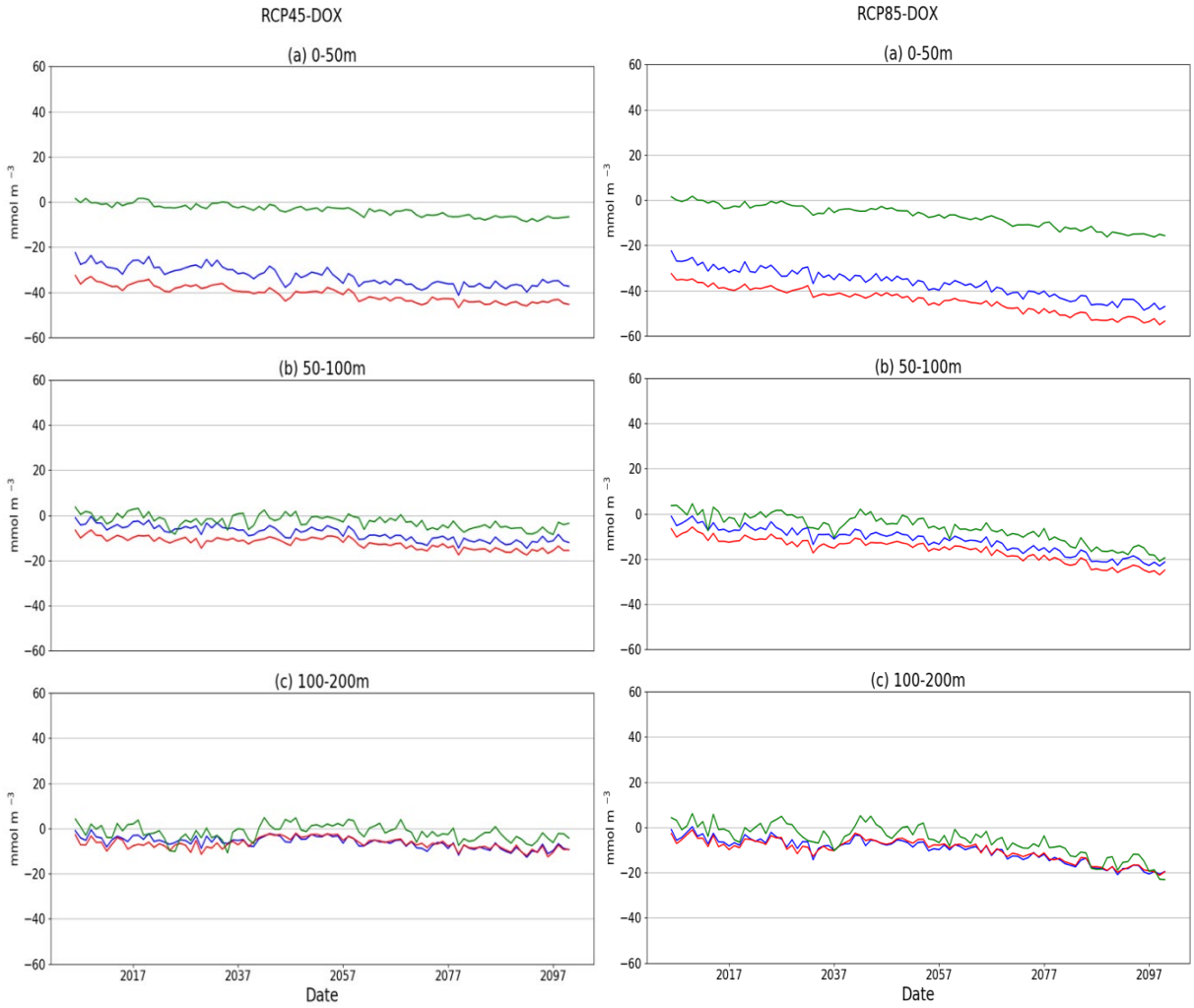

Figure 37 - Annual timeseries of dissolved oxygen anomalies (mmol/m^3) in the three inshore (depth less than 200 m) areas of the Adriatic-Ionian Sea: GSA17 - northern Adriatic (blue), GSA18 - southern Adriatic (red) and GSA19 - Ionian (green). Timeseries cover the 2005-2099 period for the two emission RCP4.5 (left) and RCP8.5 (right) scenarios.

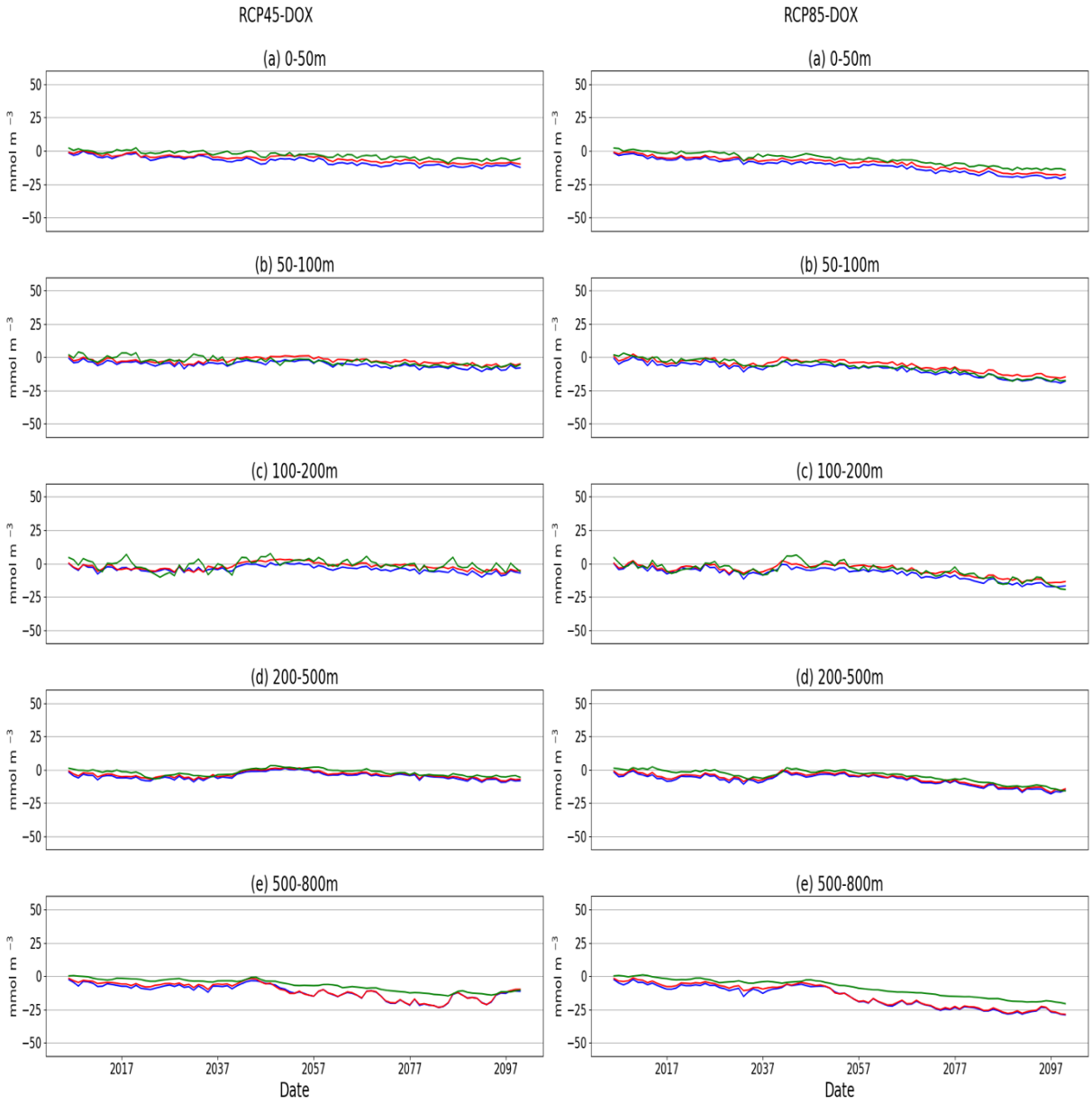

Figure 38 - Annual timeseries of dissolved oxygen anomalies (mmol/m^3) in the three offshore (deeper than 200 m) areas of the Adriatic-Ionian Sea: GSA17 - northern Adriatic (blue), GSA18 - southern Adriatic (red) and GSA19 - Ionian (green). Timeseries cover the 2005-2099 period for the two emission RCP4.5 (left) and RCP8.5 (right) scenarios.

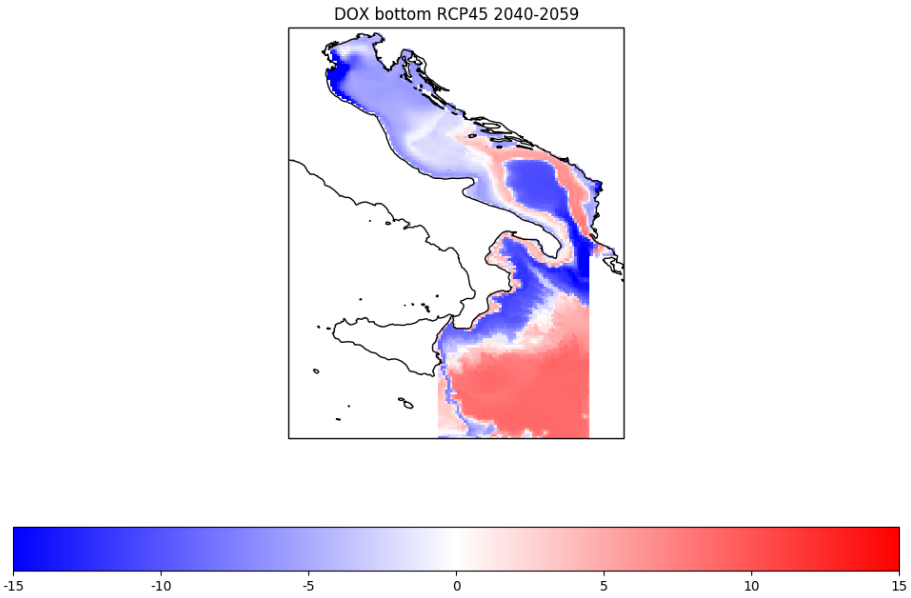

Figure 39 - Mean bottom dissolved oxygen (DOX bottom) anomalies (mmol/m^3) in the MID-FUTURE of the RCP4.5 scenario.

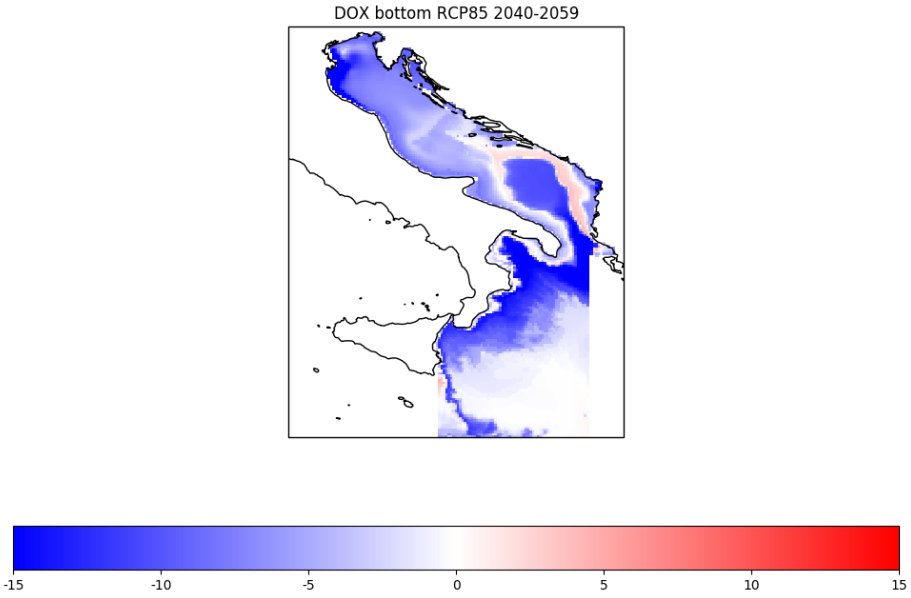

Figure 40 - Mean bottom dissolved oxygen (DOX bottom) anomalies (mmol/m^3) in the MID-FUTURE of the RCP8.5 scenario.

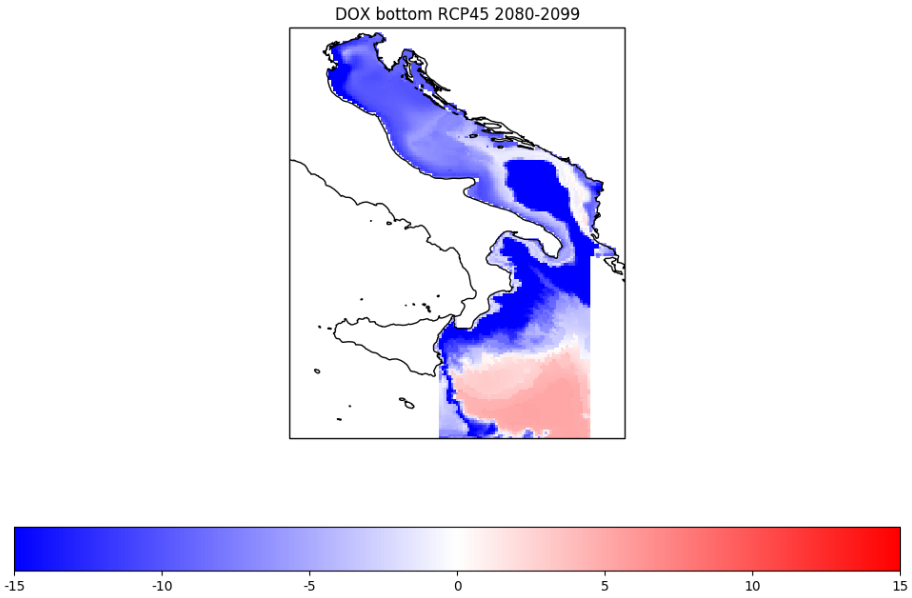

Figure 41 - Mean bottom dissolved oxygen (DOX bottom) anomalies (mmol/m^3) in the FAR-FUTURE of the RCP4.5 scenario.

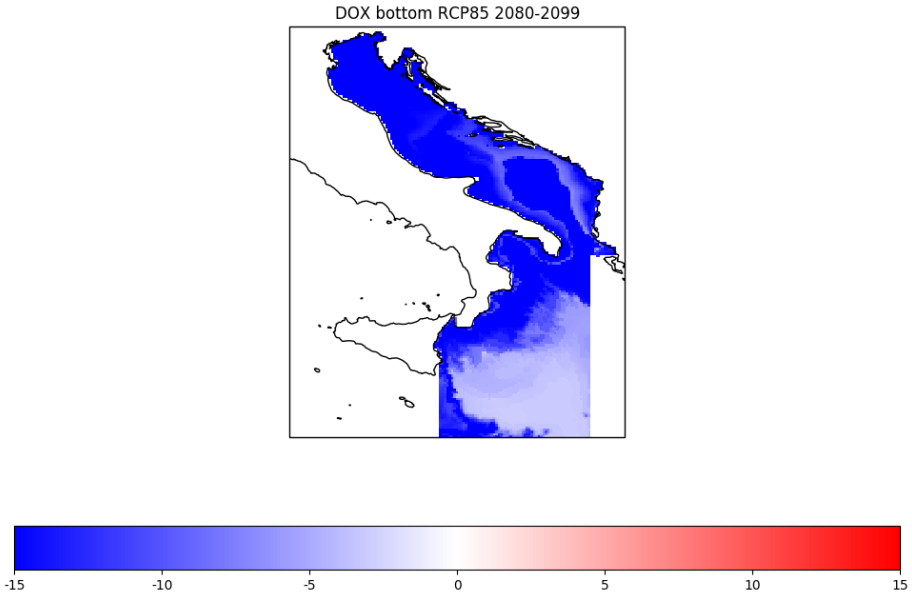

Figure 42 - Mean bottom dissolved oxygen (DOX bottom) anomalies (mmol/m^3) in the FAR-FUTURE of the RCP8.5 scenario.

pH

The acidity measurements provided by the BFM model consists of pH in total scale computed at the *in situ* condition (i.e., using temperature and pressure at the proper depth of each domain grid cell).

The pH anomalies computed for the MID-FUTURE and FAR-FUTURE under the two emission scenarios are shown in the maps of Figs. 43-46.

Decrease of pH proceeds constantly during the 21st century. Negative anomalies are higher at surface rather than subsurface layers, following both the increase of temperature and the CO_2 flux from the surface and their diffusion toward the subsurface layers.

The decrease of pH at the surface of RCP8.5 scenario, which is much stronger than RCP4.5, reaches values down to -0.3 by the end of the century.

The Figs. 47-48 show the corresponding time series of the three sub-areas in their inshore (Fig. 47) and offshore zones (Fig. 48). The negative tendencies are monotonic during the entire 21st century. Considering the different areas, the decrease of pH associated with the increase of the atmospheric CO_2 affects mainly the surface of the two basins and mainly the inshore areas (Fig.47), which appear more sensitive to the air-sea interactions.

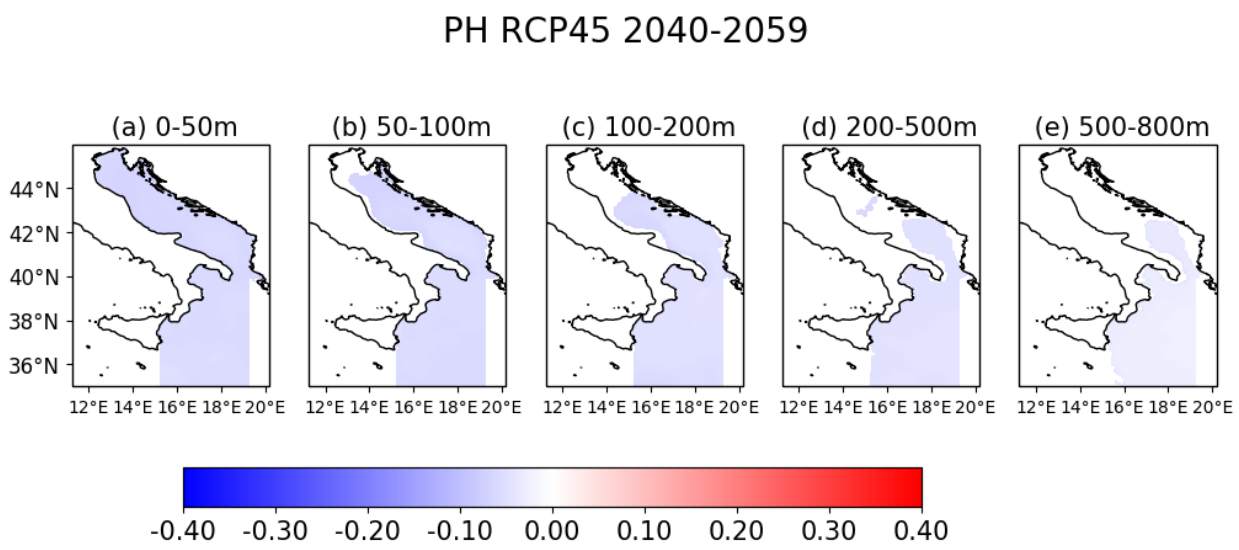

Figure 43 – Mean pH anomalies in the MID-FUTURE of the RCP4.5 scenario in the five layers: 0-50 m, 50-100 m, 100-200 m, 200-500 m and 500-800 m

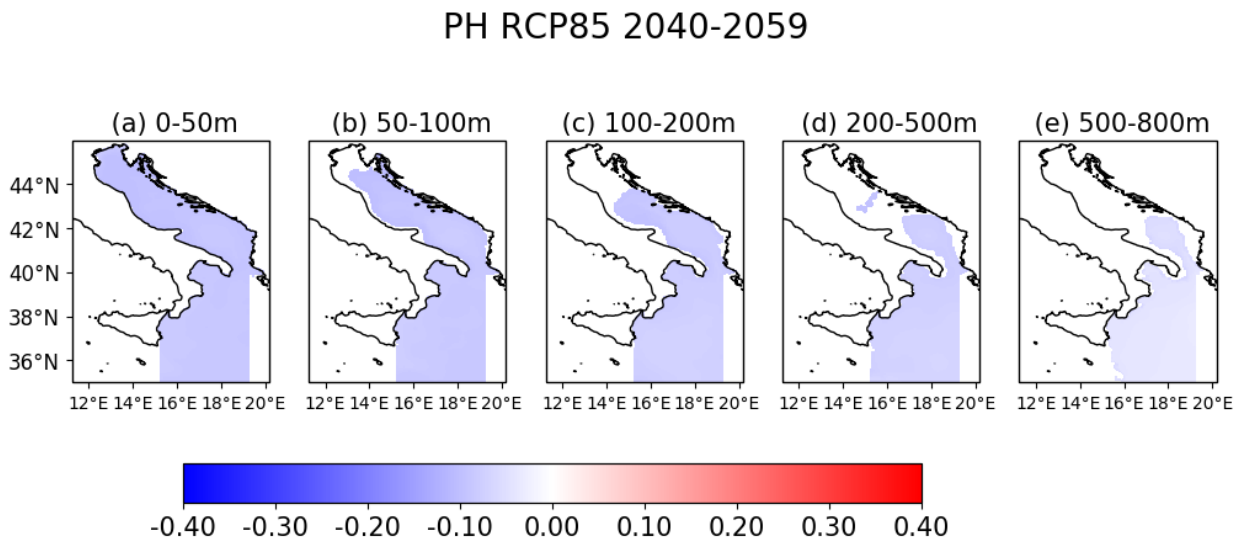

Figure 44 – Mean pH anomalies in the MID-FUTURE of the RCP8.5 scenario in the five layers: 0-50 m, 50-100 m, 100-200 m, 200-500 m and 500-800 m

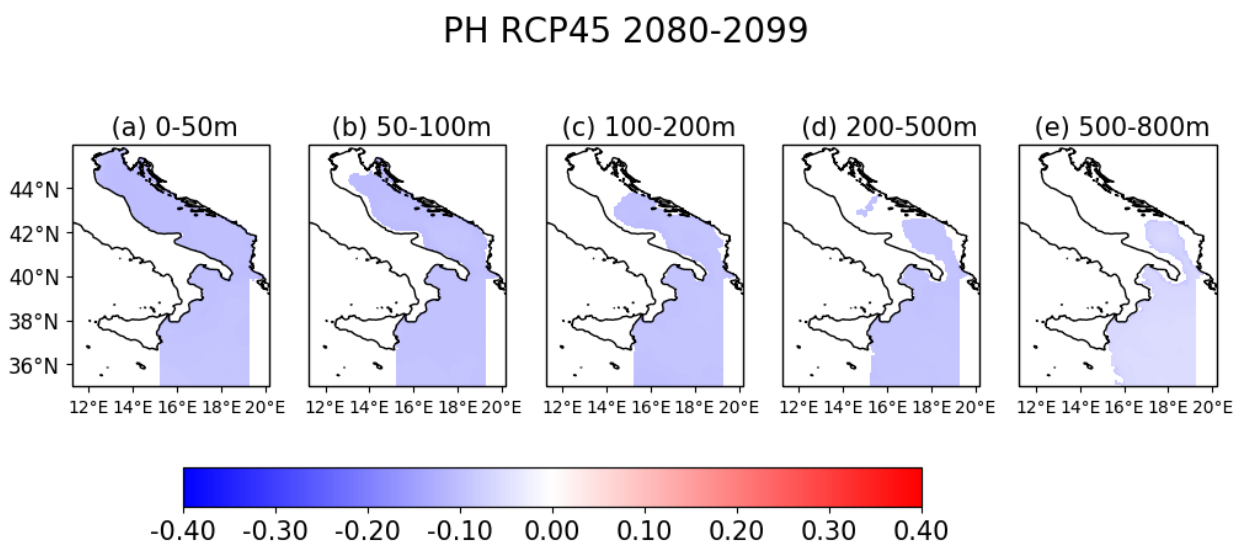

Figure 45 – Mean pH anomalies in the FAR-FUTURE of the RCP4.5 scenario in the five layers: 0-50 m, 50-100 m, 100-200 m, 200-500 m and 500-800 m

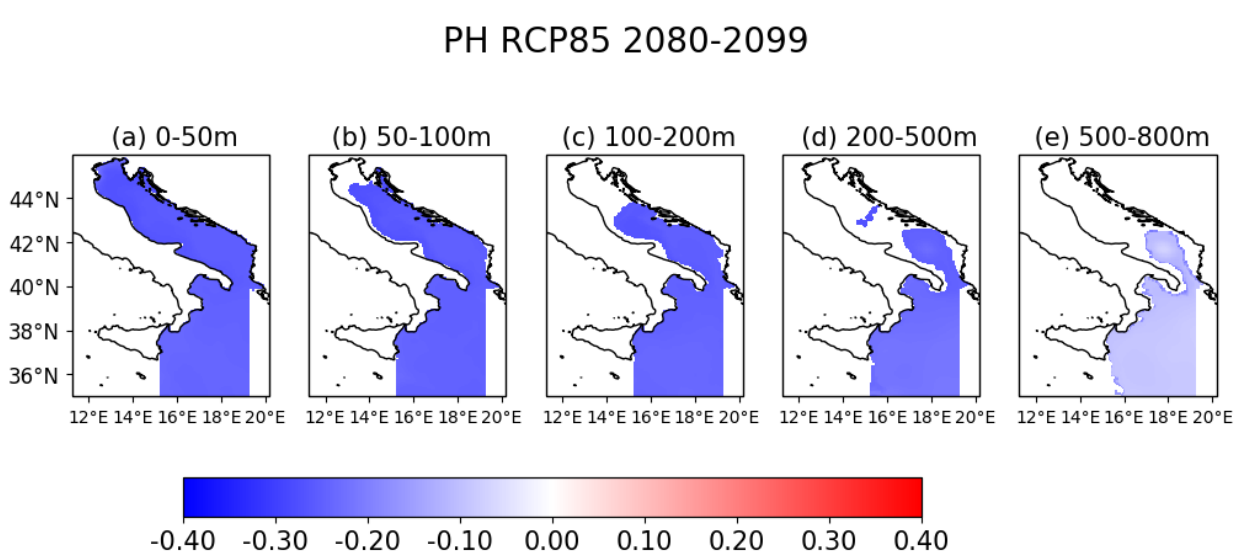

Figure 46 – Mean pH anomalies in the FAR-FUTURE of the RCP8.5 scenario in the five layers: 0-50 m, 50-100 m, 100-200 m, 200-500 m and 500-800 m

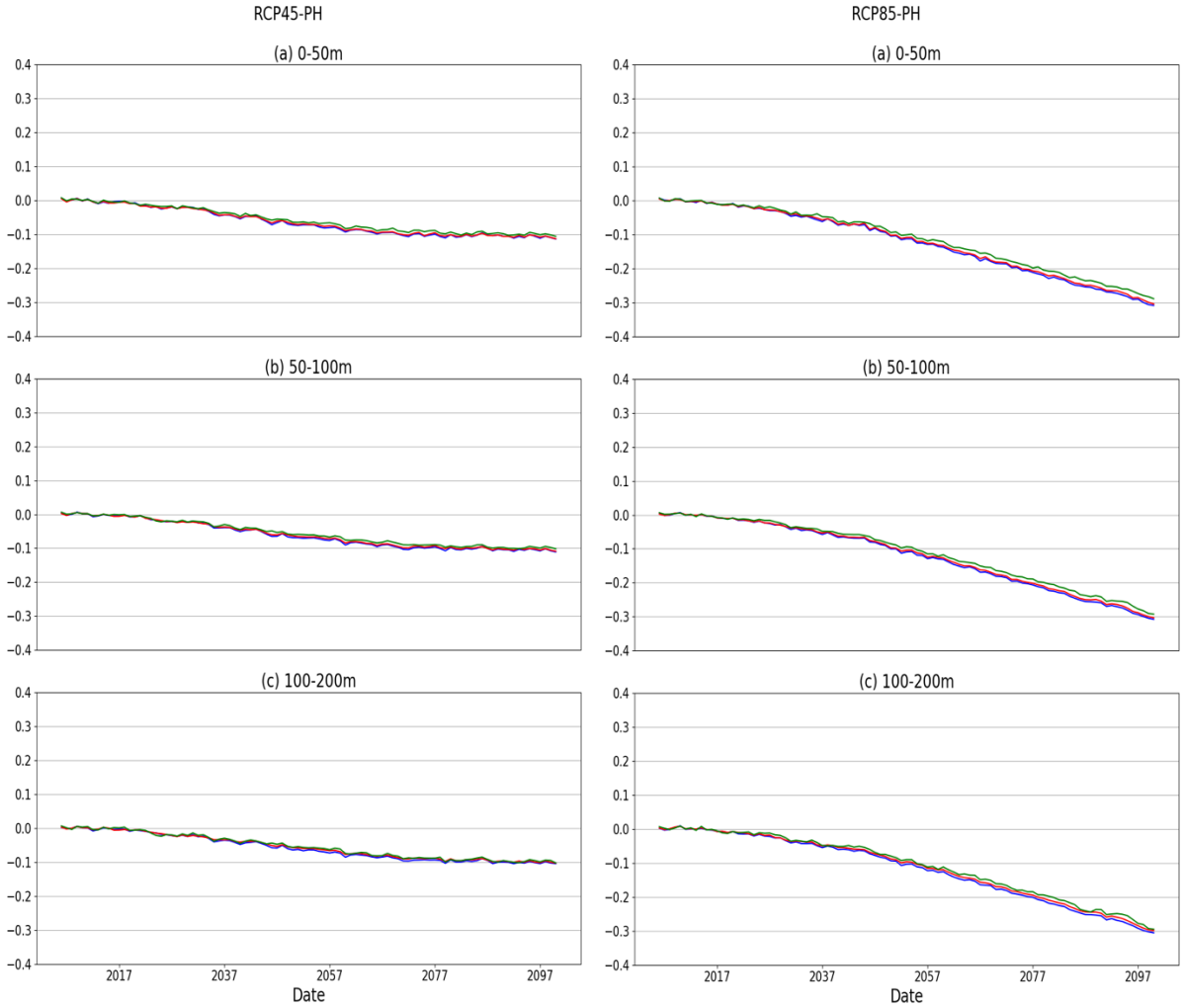

Figure 47 - Annual timeseries of pH anomalies in the three inshore (depth less than 200 m) areas of the Adriatic-Ionian Sea: GSA17 - northern Adriatic (blue), GSA18 - southern Adriatic (red) and GSA19 - Ionian (green). Timeseries cover the 2005-2099 period for the two emission RCP4.5 (left) and RCP8.5 (right) scenarios

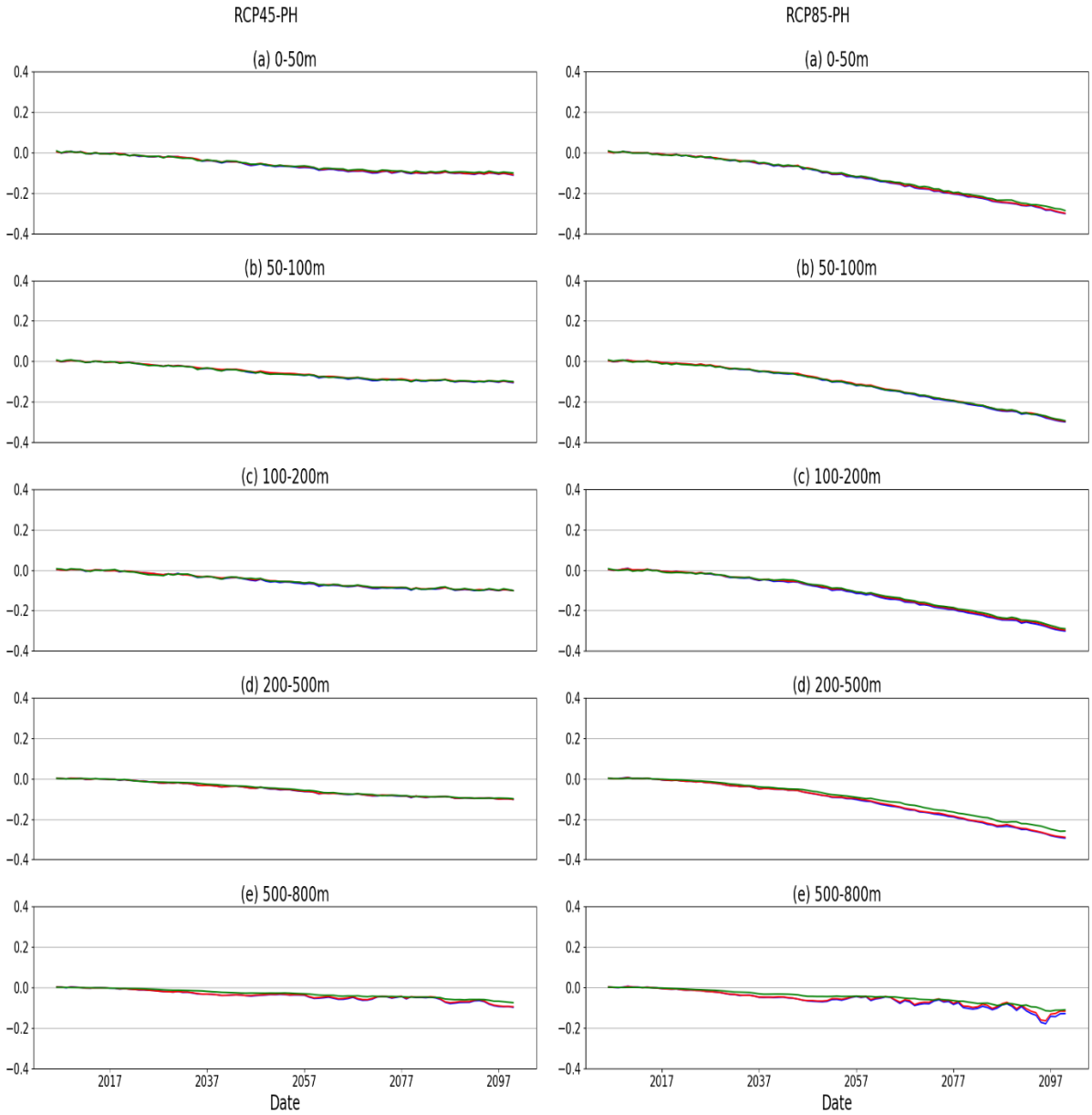

Figure 48 - Annual timeseries of pH anomalies in the three offshore (depth greater than 200 m) areas of the Adriatic-Ionian Sea: GSA17 - northern Adriatic (blue), GSA18 - southern Adriatic (red) and GSA19 - Ionian (green). Timeseries cover the 2005-2099 period for the two emission RCP4.5 (left) and RCP8.5 (right) scenarios.

Near Future evolution of biogeochemical variables

Mean values of the biogeochemical variables for the 5-year intervals of the next two decades and for the MID-FUTURE and FAR-FUTURE periods are reported in the following tables.

DIN (mmol/m^3)		PRESENT	2021 - 2025		2026 - 2030		2031 - 2035		2036 - 2040		2040 - 2059		2080 - 2099	
			RCP4.5	*RCP8.5*	RCP4.5	*RCP8.5*	RCP4.5	*RCP8.5*	RCP4.5	*RCP8.5*	RCP4.5	*RCP8.5*	RCP4.5	*RCP8.5*
ADR1	0 - 50 m	**1.31**	1.32	*1.51*	1.43	*1.21*	1.50	*1.74*	1.22	*1.22*	1.26	*1.40*	1.40	*1.45*
	50 - 100 m	**0.97**	0.91	*0.88*	0.90	*0.81*	0.95	*1.03*	0.68	*0.79*	0.61	*0.76*	0.70	*0.89*
	100 - 200 m	**1.78**	1.71	*1.72*	1.67	*1.52*	1.94	*1.94*	1.12	*1.25*	0.94	*1.16*	1.12	*1.34*
	200 - 500 m	**2.42**	2.32	*2.22*	2.28	*2.19*	2.77	*2.56*	1.82	*1.95*	1.54	*1.75*	1.77	*2.02*
	500 - 800 m	**3.36**	3.27	*3.14*	3.27	*3.26*	3.54	*3.46*	2.86	*3.15*	2.60	*2.90*	2.92	*3.33*
ADR2	0 - 50 m	**0.58**	0.48	*0.48*	0.60	*0.54*	0.45	*0.58*	0.41	*0.46*	0.25	*0.37*	0.37	*0.44*
	50 - 100 m	**1.18**	1.09	*1.12*	1.16	*1.04*	1.27	*1.34*	0.57	*0.73*	0.46	*0.66*	0.63	*0.80*
	100 - 200 m	**2.17**	2.09	*2.04*	2.07	*1.98*	2.33	*2.30*	1.33	*1.47*	1.04	*1.30*	1.35	*1.58*
	200 - 500 m	**2.93**	2.88	*2.75*	2.84	*2.79*	3.14	*3.06*	2.34	*2.49*	1.97	*2.18*	2.28	*2.47*
	500 - 800 m	**3.39**	3.29	*3.15*	3.33	*3.25*	3.52	*3.45*	2.95	*3.17*	2.73	*2.97*	3.02	*3.41*
ION	0 - 50 m	**0.21**	0.13	*0.22*	0.25	*0.22*	0.06	*0.18*	0.16	*0.16*	0.11	*0.09*	0.15	*0.05*
	50 - 100 m	**0.47**	0.45	*0.47*	0.63	*0.46*	0.24	*0.36*	0.40	*0.33*	0.22	*0.11*	0.28	*0.08*
	100 - 200 m	**1.71**	1.95	*1.46*	2.08	*1.57*	1.45	*1.31*	1.59	*1.17*	0.84	*0.46*	1.05	*0.68*
	200 - 500 m	**2.86**	3.05	*2.77*	2.86	*2.87*	3.07	*3.08*	2.67	*2.67*	2.26	*2.41*	2.43	*2.62*
	500 - 800 m	**3.58**	3.52	*3.52*	3.57	*3.57*	3.62	*3.63*	3.51	*3.59*	3.38	*3.48*	3.57	*3.75*

Table 1 - Mean values of dissolved inorganic nitrogen for the present condition (bold font), for the 5-year intervals of the next two decades and for the MID-FUTURE and FAR-FUTURE periods. For each time period in the future, both the RCP4.5 (normal font) and RCP8.5 (italic font) scenarios have been considered. Data have been subdivided into the three GSA areas: northern Adriatic (ADR1 - GSA17), southern Adriatic (ADR2 - GSA18) and Ionian (ION - GSA19). For each area, five layers with increasing depth (0-50 m, 50-100 m, 100-200 m, 200-500 m, 500-800 m) have been considered.

PO_4 (mmol/m^3)		PRESENT	2021 - 2025		2026 - 2030		2031 - 2035		2036 - 2040		2040 - 2059		2080 - 2099	
			RCP4.5	RCP8.5	RCP4.5	RCP8.5	RCP4.5	RCP8.5	RCP4.5	RCP8.5	RCP4.5	RCP8.5	RCP4.5	RCP8.5
ADR1	0 - 50 m	**0.029**	0.026	*0.031*	0.031	*0.028*	0.030	*0.031*	0.023	*0.023*	0.020	*0.022*	0.021	*0.021*
	50 - 100 m	**0.063**	0.057	*0.066*	0.061	*0.057*	0.066	*0.069*	0.042	*0.045*	0.038	*0.043*	0.042	*0.044*
	100 - 200 m	**0.113**	0.104	*0.117*	0.107	*0.101*	0.123	*0.123*	0.072	*0.076*	0.062	*0.072*	0.070	*0.078*
	200 - 500 m	**0.130**	0.118	*0.126*	0.120	*0.121*	0.146	*0.138*	0.092	*0.098*	0.074	*0.083*	0.084	*0.093*
	500 - 800 m	**0.144**	0.136	*0.139*	0.137	*0.141*	0.155	*0.153*	0.114	*0.127*	0.093	*0.108*	0.107	*0.127*
ADR2	0 - 50 m	**0.028**	0.020	*0.030*	0.030	*0.027*	0.026	*0.032*	0.013	*0.015*	0.006	*0.011*	0.011	*0.011*
	50 - 100 m	**0.075**	0.068	*0.079*	0.073	*0.069*	0.082	*0.085*	0.039	*0.043*	0.030	*0.039*	0.040	*0.043*
	100 - 200 m	**0.124**	0.118	*0.123*	0.117	*0.114*	0.133	*0.132*	0.074	*0.078*	0.055	*0.067*	0.073	*0.079*
	200 - 500 m	**0.139**	0.134	*0.135*	0.133	*0.132*	0.150	*0.148*	0.103	*0.106*	0.078	*0.087*	0.095	*0.098*
	500 - 800 m	**0.145**	0.137	*0.139*	0.140	*0.140*	0.154	*0.153*	0.118	*0.126*	0.100	*0.112*	0.113	*0.133*
ION	0 - 50 m	**0.014**	0.010	*0.018*	0.018	*0.013*	0.008	*0.012*	0.010	*0.008*	0.007	*0.006*	0.009	*0.004*
	50 - 100 m	**0.034**	0.035	*0.037*	0.044	*0.031*	0.024	*0.025*	0.034	*0.023*	0.020	*0.011*	0.024	*0.012*
	100 - 200 m	**0.096**	0.112	*0.082*	0.115	*0.084*	0.085	*0.071*	0.091	*0.059*	0.045	*0.022*	0.057	*0.038*
	200 - 500 m	**0.131**	0.145	*0.129*	0.130	*0.133*	0.144	*0.149*	0.120	*0.120*	0.097	*0.105*	0.107	*0.115*
	500 - 800 m	**0.150**	0.149	*0.150*	0.149	*0.149*	0.154	*0.157*	0.145	*0.151*	0.134	*0.140*	0.142	*0.152*

Table 2 - Same as Table 1, for phosphate.

PHYC (mgC/m^3)		PRESENT	2021 - 2025		2026 - 2030		2031 - 2035		2036 - 2040		2040 - 2059		2080 - 2099	
			RCP4.5	RCP8.5	RCP4.5	RCP8.5	RCP4.5	RCP8.5	RCP4.5	RCP8.5	RCP4.5	RCP8.5	RCP4.5	RCP8.5
ADR1	0 - 50 m	**18.2**	17.7	*18.6*	18.2	*17.6*	18.4	*18.5*	16.6	*16.8*	16.3	*16.5*	16.1	*15.7*
	50 - 100 m	**9.7**	9.1	*9.9*	9.5	*9.2*	9.9	*10.0*	7.9	*8.2*	7.4	*7.7*	7.6	*7.3*
	100 - 200 m	**1.6**	1.1	*1.7*	1.5	*1.5*	1.3	*1.9*	0.9	*1.3*	0.9	*1.0*	0.8	*0.8*
	200 - 500 m	**0.2**	0.0	*0.3*	0.3	*0.2*	0.0	*0.3*	0.0	*0.1*	0.0	*0.0*	-0.1	*-0.2*
	500 - 800 m	**0.0**	-0.1	*0.1*	0.1	*-0.1*	-0.1	*-0.1*	-0.1	*-0.3*	-0.2	*-0.2*	-0.2	*-0.3*
ADR2	0 - 50 m	**13.4**	13.0	*13.6*	13.3	*12.6*	14.0	*13.9*	11.2	*11.6*	10.8	*11.1*	10.8	*10.6*
	50 - 100 m	**9.6**	9.2	*9.7*	9.4	*9.2*	10.1	*10.0*	8.2	*8.4*	7.6	*7.8*	7.8	*7.7*
	100 - 200 m	**1.3**	1.1	*1.5*	1.3	*1.2*	1.2	*1.4*	1.2	*1.3*	1.0	*1.0*	0.9	*0.8*
	200 - 500 m	**0.2**	0.0	*0.2*	0.2	*0.1*	0.0	*0.1*	0.0	*0.0*	-0.1	*-0.1*	-0.1	*-0.2*
	500 - 800 m	**0.0**	-0.1	*0.0*	0.0	*0.0*	-0.1	*-0.1*	-0.1	*-0.1*	-0.2	*-0.1*	-0.2	*-0.2*
ION	0 - 50 m	**7.8**	7.5	*8.6*	8.5	*7.3*	6.8	*7.6*	6.9	*6.4*	6.2	*5.8*	6.2	*4.8*
	50 - 100 m	**10.1**	9.9	*10.6*	10.5	*9.9*	9.0	*9.6*	9.6	*8.6*	8.7	*7.8*	8.7	*6.8*
	100 - 200 m	**1.1**	0.8	*1.3*	1.2	*1.2*	0.9	*1.0*	1.2	*1.2*	1.2	*1.2*	1.2	*1.1*
	200 - 500 m	**0.0**	0.0	*0.1*	0.1	*0.1*	0.0	*0.0*	0.0	*0.0*	0.0	*0.0*	0.0	*0.0*
	500 - 800 m	**0.0**	0.0	*0.0*	0.0	*0.0*	0.0	*0.0*	0.0	*0.0*	0.0	*0.0*	0.0	*0.0*

Table 3 - Same as Table 1, for phytoplankton biomass.

CHL (mgChl-a/m^3)		PRESENT	2021 - 2025		2026 - 2030		2031 - 2035		2036 - 2040		2040 - 2059		2080 - 2099	
			RCP4.5	*RCP8.5*	RCP4.5	*RCP8.5*	RCP4.5	*RCP8.5*	RCP4.5	*RCP8.5*	RCP4.5	*RCP8.5*	RCP4.5	*RCP8.5*
ADR1	0 - 50 m	**0.25**	0.24	*0.25*	0.24	*0.24*	0.25	*0.25*	0.23	*0.23*	0.22	*0.23*	0.22	*0.23*
	50 - 100 m	**0.17**	0.17	*0.18*	0.17	*0.17*	0.18	*0.19*	0.15	*0.15*	0.14	*0.15*	0.15	*0.16*
	100 - 200 m	**0.05**	0.04	*0.05*	0.05	*0.05*	0.05	*0.06*	0.04	*0.05*	0.04	*0.04*	0.04	*0.05*
	200 - 500 m	**0.01**	0.00	*0.01*	0.01	*0.01*	0.00	*0.01*	0.01	*0.01*	0.00	*0.00*	0.00	*0.00*
	500 - 800 m	**0.00**	0.00	*0.00*	0.00	*0.00*	0.00	*0.00*	0.00	*-0.01*	-0.01	*-0.01*	-0.01	*-0.01*
ADR2	0 - 50 m	**0.17**	0.17	*0.18*	0.17	*0.16*	0.18	*0.18*	0.15	*0.16*	0.14	*0.15*	0.14	*0.15*
	50 - 100 m	**0.16**	0.16	*0.16*	0.16	*0.16*	0.17	*0.17*	0.14	*0.15*	0.13	*0.14*	0.14	*0.16*
	100 - 200 m	**0.04**	0.04	*0.05*	0.04	*0.04*	0.04	*0.05*	0.04	*0.05*	0.04	*0.04*	0.04	*0.04*
	200 - 500 m	**0.01**	0.00	*0.01*	0.01	*0.01*	0.00	*0.01*	0.00	*0.00*	0.00	*0.00*	0.00	*0.00*
	500 - 800 m	**0.00**	0.00	*0.00*	0.00	*0.00*	0.00	*0.00*	0.00	*0.00*	-0.01	*-0.01*	-0.01	*-0.01*
ION	0 - 50 m	**0.09**	0.09	*0.10*	0.10	*0.09*	0.08	*0.09*	0.08	*0.08*	0.07	*0.07*	0.08	*0.06*
	50 - 100 m	**0.13**	0.13	*0.14*	0.15	*0.13*	0.11	*0.13*	0.13	*0.12*	0.12	*0.11*	0.13	*0.11*
	100 - 200 m	**0.03**	0.02	*0.03*	0.03	*0.03*	0.02	*0.03*	0.03	*0.03*	0.03	*0.03*	0.04	*0.04*
	200 - 500 m	**0.00**	0.00	*0.00*	0.00	*0.00*	0.00	*0.00*	0.00	*0.00*	0.00	*0.00*	0.00	*0.00*
	500 - 800 m	**0.00**	0.00	*0.00*	0.00	*0.00*	0.00	*0.00*	0.00	*0.00*	0.00	*0.00*	0.00	*0.00*

Table 4 - Same as Table 1, for chlorophyll.

NPP (mgC/m^3/day)		PRESENT	2021 - 2025		2026 - 2030		2031 - 2035		2036 - 2040		2040 - 2059		2080 - 2099	
			RCP4.5	*RCP8.5*	RCP4.5	*RCP8.5*	RCP4.5	*RCP8.5*	RCP4.5	*RCP8.5*	RCP4.5	*RCP8.5*	RCP4.5	*RCP8.5*
ADR1	0 - 50 m	**10.44**	10.29	*10.54*	10.47	*10.57*	10.42	*10.63*	10.31	*10.38*	10.14	*10.31*	10.43	*10.94*
	50 - 100 m	**0.45**	0.45	*0.46*	0.49	*0.50*	0.48	*0.48*	0.48	*0.47*	0.44	*0.47*	0.55	*0.66*
	100 - 200 m	**-0.15**	-0.12	*-0.16*	-0.14	*-0.15*	-0.13	*-0.17*	-0.11	*-0.14*	-0.11	*-0.12*	-0.11	*-0.12*
	200 - 500 m	**-0.02**	-0.01	*-0.03*	-0.03	*-0.02*	-0.01	*-0.03*	-0.02	*-0.02*	-0.01	*-0.01*	-0.01	*-0.01*
	500 - 800 m	**0.00**	0.01	*-0.01*	0.00	*0.00*	0.00	*0.00*	0.01	*0.02*	0.01	*0.01*	0.01	*0.02*
ADR2	0 - 50 m	**8.92**	8.78	*9.06*	9.02	*8.97*	9.01	*9.13*	8.63	*8.78*	8.36	*8.60*	8.77	*9.35*
	50 - 100 m	**0.69**	0.68	*0.71*	0.73	*0.74*	0.74	*0.74*	0.70	*0.72*	0.67	*0.74*	0.83	*1.06*
	100 - 200 m	**-0.13**	-0.11	*-0.14*	-0.13	*-0.13*	-0.12	*-0.14*	-0.12	*-0.13*	-0.11	*-0.12*	-0.11	*-0.11*
	200 - 500 m	**-0.02**	-0.01	*-0.02*	-0.02	*-0.02*	-0.01	*-0.01*	-0.01	*-0.01*	0.00	*0.00*	0.00	*0.00*
	500 - 800 m	**0.00**	0.01	*0.00*	0.00	*0.00*	0.00	*0.00*	0.01	*0.01*	0.01	*0.01*	0.01	*0.01*
ION	0 - 50 m	**6.13**	6.02	*6.52*	6.46	*6.20*	5.72	*6.30*	6.02	*5.95*	5.85	*5.85*	6.32	*6.57*
	50 - 100 m	**0.90**	0.97	*0.98*	1.01	*1.00*	0.80	*1.03*	0.97	*0.96*	0.95	*0.95*	1.14	*1.38*
	100 - 200 m	**-0.02**	0.00	*-0.03*	-0.03	*-0.02*	0.00	*-0.01*	-0.01	*0.00*	0.00	*0.01*	0.01	*0.07*
	200 - 500 m	**0.00**	0.00	*-0.01*	-0.01	*-0.01*	0.00	*0.00*	0.00	*0.00*	0.00	*0.00*	0.00	*0.00*
	500 - 800 m	**0.00**	0.00	*0.00*	0.00	*0.00*	0.00	*0.00*	0.00	*0.00*	0.00	*0.00*	0.00	*0.00*

Table 5 - Same as Table 1, for net primary production.

DOX (mmol/m^3)		PRESENT	2021 - 2025		2026 - 2030		2031 - 2035		2036 - 2040		2040 - 2059		2080 - 2099	
			RCP4.5	*RCP8.5*	RCP4.5	*RCP8.5*	RCP4.5	*RCP8.5*	RCP4.5	*RCP8.5*	RCP4.5	*RCP8.5*	RCP4.5	*RCP8.5*
ADR1	0 - 50 m	**225.9**	221.2	*223.0*	226.4	*223.4*	222.8	*219.5*	221.5	*221.0*	220.0	*218.2*	215.9	*208.4*
	50 - 100 m	**227.1**	225.8	*227.3*	225.3	*223.7*	227.1	*223.9*	222.8	*222.4*	224.1	*222.1*	219.5	*211.8*
	100 - 200 m	**222.4**	221.3	*222.8*	221.0	*220.1*	221.7	*218.5*	220.6	*220.0*	222.7	*220.2*	217.5	*209.4*
	200 - 500 m	**218.3**	216.9	*218.9*	218.0	*216.0*	217.6	*213.8*	216.9	*215.9*	220.3	*217.4*	214.7	*206.4*
	500 - 800 m	**205.8**	204.5	*206.4*	204.6	*202.7*	204.1	*202.0*	204.3	*201.8*	204.5	*201.7*	197.1	*187.2*
ADR2	0 - 50 m	**222.4**	220.8	*221.8*	220.4	*219.6*	222.0	*219.7*	218.3	*217.8*	219.2	*217.4*	214.8	*208.4*
	50 - 100 m	**221.8**	220.4	*221.4*	220.1	*219.8*	220.8	*217.9*	221.2	*220.0*	222.8	*220.1*	217.7	*209.8*
	100 - 200 m	**216.9**	215.1	*216.8*	215.8	*215.4*	215.5	*213.0*	217.9	*216.9*	221.0	*217.7*	214.9	*206.6*
	200 - 500 m	**210.2**	208.3	*210.0*	209.3	*208.5*	208.3	*206.6*	210.3	*209.7*	214.2	*211.2*	208.0	*200.5*
	500 - 800 m	**204.1**	202.4	*204.1*	203.0	*201.3*	201.9	*200.3*	202.8	*200.3*	200.9	*198.4*	193.4	*183.7*
ION	0 - 50 m	**216.7**	215.9	*216.7*	215.7	*215.2*	216.5	*213.2*	214.8	*213.2*	214.3	*212.5*	210.4	*204.4*
	50 - 100 m	**220.4**	217.4	*220.2*	217.8	*218.8*	221.4	*215.9*	217.4	*215.1*	217.9	*216.7*	214.0	*205.6*
	100 - 200 m	**210.4**	204.2	*212.3*	205.6	*210.8*	210.0	*208.6*	207.2	*207.9*	213.5	*213.6*	208.0	*200.0*
	200 - 500 m	**203.2**	198.9	*203.0*	201.1	*201.1*	199.9	*198.0*	201.0	*199.1*	205.8	*202.6*	199.8	*191.4*
	500 - 800 m	**197.1**	196.2	*197.1*	195.7	*193.1*	195.7	*194.4*	194.5	*192.9*	194.1	*192.2*	186.3	*180.0*

Table 6 - Same as Table 1, for dissolved oxygen.

pH		PRESENT	2021 - 2025		2026 - 2030		2031 - 2035		2036 - 2040		2040 - 2059		2080 - 2099	
			RCP4.5	*RCP8.5*	RCP4.5	*RCP8.5*	RCP4.5	*RCP8.5*	RCP4.5	*RCP8.5*	RCP4.5	*RCP8.5*	RCP4.5	*RCP8.5*
ADR1	0 - 50 m	**8.13**	8.11	*8.11*	8.11	*8.09*	8.10	*8.08*	8.08	*8.07*	8.06	*8.03*	8.02	*7.87*
	50 - 100 m	**8.14**	8.13	*8.13*	8.12	*8.11*	8.11	*8.10*	8.10	*8.08*	8.08	*8.05*	8.04	*7.88*
	100 - 200 m	**8.14**	8.13	*8.13*	8.12	*8.11*	8.11	*8.10*	8.10	*8.09*	8.08	*8.05*	8.04	*7.88*
	200 - 500 m	**8.13**	8.13	*8.12*	8.12	*8.11*	8.11	*8.10*	8.10	*8.08*	8.08	*8.05*	8.04	*7.88*
	500 - 800 m	**8.11**	8.10	*8.10*	8.09	*8.09*	8.09	*8.08*	8.08	*8.06*	8.07	*8.05*	8.04	*7.98*
ADR2	0 - 50 m	**8.11**	8.10	*8.10*	8.10	*8.09*	8.09	*8.08*	8.07	*8.06*	8.06	*8.02*	8.02	*7.86*
	50 - 100 m	**8.13**	8.12	*8.12*	8.11	*8.11*	8.11	*8.10*	8.09	*8.08*	8.08	*8.05*	8.04	*7.88*
	100 - 200 m	**8.13**	8.12	*8.12*	8.11	*8.10*	8.10	*8.09*	8.09	*8.08*	8.08	*8.05*	8.03	*7.88*
	200 - 500 m	**8.12**	8.11	*8.11*	8.10	*8.10*	8.10	*8.09*	8.09	*8.07*	8.07	*8.04*	8.03	*7.88*
	500 - 800 m	**8.11**	8.10	*8.10*	8.09	*8.09*	8.09	*8.08*	8.08	*8.06*	8.08	*8.06*	8.04	*8.00*
ION	0 - 50 m	**8.09**	8.09	*8.08*	8.08	*8.07*	8.07	*8.06*	8.06	*8.04*	8.04	*8.01*	8.00	*7.85*
	50 - 100 m	**8.12**	8.11	*8.11*	8.10	*8.10*	8.10	*8.09*	8.08	*8.07*	8.07	*8.04*	8.03	*7.88*
	100 - 200 m	**8.12**	8.11	*8.12*	8.10	*8.10*	8.10	*8.10*	8.09	*8.08*	8.08	*8.05*	8.03	*7.88*
	200 - 500 m	**8.12**	8.11	*8.11*	8.10	*8.10*	8.10	*8.09*	8.09	*8.08*	8.07	*8.05*	8.03	*7.90*
	500 - 800 m	**8.11**	8.10	*8.10*	8.10	*8.09*	8.10	*8.09*	8.09	*8.08*	8.08	*8.07*	8.05	*8.02*

Table 7 - Same as Table 1, for seawater acidity.

Dataset and file format of biogeochemical variables

The original data from the two simulations have been processed as described in the previous sections. The resulting statistics have been organized in NetCDF files for the specific implementation of the integrated platform of WP4. The chosen standard (NetCDF) allows for a widespread use of the results in all FAIRSEA work packages. In fact, NetCDF (Network Common Data Form) files are self-describing (i.e., they include information about the data they contain), architecture-independent (i.e., they can be accessed by computers with different ways of storing integers, characters, and floating-point numbers), appendable (i.e., data can be easily appended to a NetCDF dataset) and sharable (i.e., multiple users can simultaneously access the same NetCDF file). NetCDF data can be browsed and analyzed through a number of software, like NCO, IDL, MATLAB, PYTHON, cdo, and ncl.

In the dataset some files are named X_PERIOD_SCENARIO.nc where X can be DIN (dissolved nitrogen), N1p (phosphate), O2o (dissolved oxygen), PH (pH), ppn (net primary production), PC (phytoplankton carbon biomass), P_l (chlorophyll-a), R6c (particulate organic carbon or POC) and ZC (zooplankton carbon biomass), PERIOD can be 2021-2025, 2026-2030, 2031-2040, 2040-2059 and 2080-2099 while SCEN is the scenario (RCP4.5 and RCP8.5) .Each file contains the 2D annual anomaly X_ANOM between 0-50 m (for example anom_0m_50m), between 50-100 m (for example anom_50m_100m), between 100-200 m (for example anom_100m_200m), between 200-500 m (for example anom_200m_500m) and between 500-800 m (for example anom_500m_800m), the 2D standard deviation of the anomaly (for example std_0m_50m) and the 2D annual mean (for example mean_0m_50m) . The latter is defined as X_ANOM+X_REA where X_REA is the value of X already discussed in the

deliverable of the present state 4.2.1. Each file has a dimension of 3 MB. Table 8 shows the dimensions and variables included in the NetCDF files.

SIZE	VARIABLES		
lon=144 lat=176	**NAME**	**DIMENSIONS**	**TYPE**
	Lon	lon	Float32
	Lat	lat	Float32
	mean_0m_50m	lat, lon	double
	mean_50m_100m	lat, lon	double
	mean_100m_200m	lat, lon	double
	mean_200m_500m	lat, lon	double
	mean_500m_800m	lat, lon	double
	anom_0m_50m	lat, lon	double
	anom_50m_100m	lat, lon	double
	anom_100m_200m	lat, lon	double
	anom_200m_500m	lat, lon	double
	anom_500m_800m	lat, lon	double
	std_0m_50m	lat, lon	double
	std_50m_100m	lat, lon	double
	std_100m_200m	lat, lon	double
	std_200m_500m	lat, lon	double
	std_500m_800m	lat, lon	double

Table 8 - Dimensions and variables included in the NetCDF files

In the dataset, some other files are named Xbottom_PERIOD_SCEN.nc where X can be O2o, dissolved oxygen at the bottom, PERIOD can be 2021-2025, 2026-2030, 2031-2040, 2040-2059 and 2080-2099 while SCEN is the scenario (RCP4.5 and RCP8.5). Each file contains the 2D annual anomaly for X at the bottom, its standard deviation and the annual mean defined as X_ANOM+X_REA where X_REA is discussed in the deliverable of the present climate 4.1.1 and 4.2.1 . Each file has a size of 0.8 MB. Table 9 shows the dimensions and variables included in these NetCDF files.

SIZE	VARIABLES		
lon=144 lat=176	**NAME**	**DIMENSIONS**	**TYPE**
	Lon	lon	Float32
	Lat	lat	Float32
	mean	lat, lon	double
	std	lat, lon	double
	anom	lat, lon	double

Table 9 - Dimensions and variables included in the NetCDF files

References

Cavicchia L., Gualdi S., Sanna A., Oddo P., 2015:" The Regional Ocean Atmosphere Coupled Model COSMONEMO_MFS", CMCC Report, n RP0254, http://www.cmcc.it/publications/rp0254-the-regionalocean-atmosphere-coupled-model-cosmo-nemo_mfs

Cossarini, G., Lazzari, P., & Solidoro, C. (2015). Spatiotemporal variability of alkalinity in the Mediterranean Sea. Biogeosciences, 12(6).

Dee, D. P., et al. (2011), The ERA-Interim reanalysis: Configuration and performance of the data assimilation system, Q. J. R. Meteorol. Soc.,137, 553–597.

IPCC, 2014: AR5 *Climate Change 2014: Synthesis Report. Contribution of Working Groups I, II and III to the Fifth Assessment Report of the Intergovernmental Panel on Climate Change*.

Lazzari, P et al. (2012): Seasonal and inter-annual variability of plankton chlorophyll and primary production in the Mediterranean Sea: a modelling approach, Biogeosciences, 9, 217-233, doi:10.5194/bg-9-217-2012.

Lazzari P., G Mattia, C Solidoro, S Salon, A Crise, M Zavatarelli, P Oddo, M Vichi (2014) The impacts of climate change and environmental management policies on the trophic regimes in the Mediterranean Sea: Scenario analyses, Journal of Marine Systems.

Lazzari, P et al. (2016): Spatial variability of phosphate and nitrate in the Mediterranean Sea: A modeling approach Deep Sea Research Pages 39-52.

Moss, R. H., Edmonds, J. A., Hibbard, K. A., Manning, M. R., Rose, S. K., Van Vuuren, D. P., Meehl, G. A. (2010). The next generation of scenarios for climate change research and assessment. Nature, 463(7282), 747-756.

Oddo, P., Adani, M., Pinardi, N., Fratianni, C., Tonani, M., & Pettenuzzo, D. (2009). A nested Atlantic-Mediterranean Sea general circulation model for operational forecasting. Ocean Science, 5, 461–473. https://doi.org/10.5194/os-5-461-2009.